THE UNIVERSITY *of* EDINBURGH
Edinburgh Medical School

Biomedical Sciences

Title of Assessment: Dissertation

Examination Number: B139763

Please use this number as your "Submission Title" in Learn when you submit your essay online.

Course Name: Integrative Neuroscience

Word count: 7921

The relationship between structural and functional networks in *C. elegans*

Contents

Abstract

Neural networks process information in ways single neurons cannot. Among other processes, they integrate sensory inputs to generate holistic experiences, and they allow those sensory processes to interact with behaviour. Within the concept of neural network, we can distinguish between structural and functional networks. The former refers to physical connections - what is now called the connectome - and the latter refers to activity correlations: what neurons predict the activation or inhibition of what other neurons? But how are structural and functional networks related? I hypothesized that as one structure can give rise to different functional activity patterns, structural and functional networks should be correlated but they shouldn't be identical. I explored this relationship using the nematode *C. elegans*, the only organism for which we have a fully mapped connectome. Using its neural structure, I developed three simulators of neural network activity dynamics (pharyngeal, somatic and whole) in python, I executed pharyngeal and somatic simulators to gather temporal sequences of neural activity, I used those activities to build functional networks through Granger Causality analysis, and finally, I compared those functional networks to their underlying neural structures. Results showed significant categorical correlations comparing the existence of excitatory and inhibitory connections, and a positive correlation comparing synaptic weights in the somatic system (inhibitory connections r=0.34, excitatory r=0.31. In conclusion, functional and structural neural networks were related, but different. This supports the idea that different activity dynamics can emerge on a single structure due to indirect pathways.

Introduction

The network perspective in neuroscience has gained relevance in the last few years as methodologies, techniques and theories for acquiring and analysing neuroscientific data have been developed (Bassett & Sporns, 2017). The growth of connectomics, high-throughput tracing, fMRI and calcium imaging, among other techniques, and the advance of computational capabilities to store, process and analyse large amounts of data have fostered scientific knowledge about how brain networks are supporting cognition and behaviour. Nowadays we can explore how those simple elements -neurons- we have studied for a long time interact with each other to generate dynamic patterns of activity (Sporns, 2011a). As Rafael Yuste proposed, now it seems to be the time to change our scope from the neuron doctrine to the neural network perspective (Yuste, 2015).

Biological **neural networks** (hereafter called 'neural networks') allow living organisms to process information in a way independent neurons cannot. They integrate environmental information through sensors of different modalities, generate holistic experiences and allow the interaction between sensory information and behavioural responses (Sporns, 2011a). They can give rise to complex cognitive processes and consciousness. They are also relevant during childhood as neural network development determine future neural responses and individual capacities.

From the translational point of view, the network perspective has been helpful to understand the pathogenesis, diagnosis and treatment of several brain disorders (Bullmore & Sporns, 2009). In particular, disconnection syndromes as apraxia, alexia and aphasia (Catani & Ffytche, 2005) where there is a lack of interaction between different sensory processes and motor responses. Researchers are also using this framework to study diseases such as Alzheimer´s disease (Delbeuck, Van der Linden, & Collete, 2003; Sanz-Arigita et al., 2010) and schizophrenia (Friston, Brown, Siemerkus, & Stephan, 2016).

When studying neural networks, we can differentiate between structural and functional networks. Structural ones refer to the physical connections between neurons - nowadays called the connectome -. A description should include trigger and target neurons, and the number and size of synapses. Functional networks refer to activity correlations between neurons. In other words, which neurons predict the activation or inhibition of which other neurons. Therefore, in a structural network, two neurons are connected if there is a synapse between them. While in a functional network, two neurons are connected if their activity patterns correlate. Previous research has shown that the relationship between structural and functional networks is not straightforward (Ford & Kensinger, 2014; Park & Friston, 2013; Sporns,

2011b, 2013; Uddin, 2013). The same pattern of structural neural connections can give raise to different activity dynamics as a consequence of the existence of parallel pathways connecting neurons (i.e. chemical and electrical, direct and indirect pathways) or neuromodulation (Bargmann & Marder, 2013).

Most of the knowledge we have today about neural networks come from decades of functional studies. Nowadays, lots of resources are being invested in advancing research in connectomics. Projects as the Human Connectome Project in USA, the Brainnetome Project in China and the CONNECT project in Europe (Johansen-Berg, 2013) have optimistic prospects claiming that they will be able to offer a more accurate parcellation of brain regions and networks, to characterize network variability among individuals, and eventually, to correlate that variability with cognitive and behavioural phenotypes (Van Essen & Ugurbil, 2012).

However, I think that it is likely that neither structure nor function alone will fully explain individual variability in cognition, behaviour and brain disorders, but we need to include in the explanations the role of structural-functional interactions. Several authors support this position and claim that deciphering the relationship between structure and function in neural networks has become one of the most important contemporary challenges in neuroscience (Azulay, Itskovits, & Zaslaver, 2016; Bullmore & Sporns, 2009; Galán, 2008; Park & Friston, 2013; Seung, 2011).

In trying to provide answers for these question, I will use the *C. elegans* neural network as a model to study some interactions between structural and functional networks. I chose this model for three reasons. First, it is the only organism for which we have a full map of its connectome (White, Southgate, Thomson, & Brenner, 1986), and whose information is publicly available online. Second, because I want to maintain structural accuracy coming from Electron Microscopy imaging, avoiding indirect structural mappings coming from tensor diffusion imaging or tractography (Greicius, Supekar, Menon, & Dougherty, 2009; Honey et al., 2009). Third, the low number of neurons and connections in its connectome allow a deeper analysis and to use limited computational resources.

Caenorhabditis elegans is a tiny nematode of about 1 mm body length that has been used for a long time as research model in biology. In 1986, it attracted the attention of neuroscientific community because its whole connectome was reconstructed and published (White et al., 1986). The hermaphrodite connectome consists of 302 neurons wired by gap junctions and chemical synapses, the latter working as inhibitory and excitatory connections. Among the neurotransmitters involved in those synapses we can find Glutamate, Acetylcholine, Dopamine, Serotonin and GABA.

We should note that, *C. elegans* neurons' do not fire action potentials, instead they react to inputs with non-linear responses called graded potentials (Goodman, Hall, Avery, & Lockery, 1998). *C. elegans* depolarizations' peak depends on the intensity of the stimulus and they don't have an intrinsic decay, its depolarization remains until the end of the stimulation (Mellem, Brockie, Madsen, & Maricq, 2009).

In this connectome, we can differentiate two neural systems connected by a pair of interneurons: a pharyngeal system, with 20 neurons dedicated to feeding processes whose cells are directly next to the muscles they control, and a somatic system with 282 neurons that controls behaviours related to whole body movement and whose neurons are separated from the muscles by a basal lamina (Altun & Hall, 2011).

Previous research has analysed the somatic system's network structure pointing out several features (Varshney, Chen, Paniagua, Hall, & Chklovskii, 2011). For three of its neurons (CANL, CANR and VC06) haven't been reported connections to any other neuron, and other five are very isolated (IL2DL, IL2DR, PLNR, DD06 and PVDR). The network has properties of a small world network, meaning that it maintains a strong clustering coefficient (C = 0.26) so nodes tend to link together generating mostly isolated communities, but at the same time, the path length is not high (L = 2.87), so some connections allow an easy communication between those isolated groups (Watts & Strogatz, 1998). These properties make information processing more efficient in a network.

The neural activity I will use to compose functional networks will be simulated with our own algorithms. I chose this computational approach first, because we need to identify with accuracy each neuron during activity measurement and just obtaining electrophysiological recordings from *C. elegans* has been challenging due to its body structure and neuron size (Schafer, 2006). Additionally, a computational approach avoids errors in activity measurements or related to strange variables' interactions. Moreover, a detailed exploration of what specific features can make structural and functional networks to defer, can become more insightful if we have the chance to manipulate the underlying structural network - what's easier with modelling -.

Aims

Our general aim was to explore the relationship between structural and functional networks in *C. elegans*. To do it, I tackled the following objectives: **First**, curate a basic simulator for *C. elegans* neural network

(Cao, 2017) with biological data maintaining an inexpensive computational design. **Second,** validate network activity against electrophysiological recordings. **Third,** characterize the behaviour of simulator's parameters regarding variables such as activity persistence, minimum node activity, attenuated potentials and sensory stimulation. **Fourth**, gather datasets of simulated activity and fit them generalized linear models predicting each neuron's activation based on the activation of all the other neurons. **Fifth**, measure the connectivity strength of each pair of neurons' in the network. **Sixth,** test the statistical significance of each connection. **Seventh,** compare Granger analysis' significant connections to the existence of excitatory and inhibitory synapses in the structural network, calculating sensitivity, specificity and categorical correlation. **Eighth,** compare Granger analysis predicted connection weights with structural weights and explore their correlation. **Ninth,** compare results between somatic system and pharynx system networks.

I **hypothesize first** that it is possible to generate a model for neural activity dynamics that while being computationally cheap, it is a valid reproduction of *C. elegans* neural activity. Our **second hypothesis** is that functional network predictions of connections' existence will be positively correlated to the existence of actual structural connections but will not be identical. Our **third hypothesis** is that not only the existence, but also the strength of connections will be positively correlated but will not be identical. Our **fourth hypothesis** is that the correlations between structural and functional connectivity will be lower as the complexity in the analysed network raises and therefore the existence of alternative pathways. Thus, the somatic system's correlation between structural and functional networks will be will lower compared to the pharynx system's correlations.

Methods

Data about the *C. elegans* connectome comes from the following online resources: WormAtlas for cells types, sensor types and main neurotransmitters used (Altun & Hall, 2011); WormWiring for structural network data with connections, weights and connection types (Jarrell et al., 2012); and OpenWorm project for 3D cell positions (Gleeson, Lung, Grosu, Hasani, & Larson, 2018). I implemented this data in our simulators.

Network simulators

I developed three simulators: one for the pharyngeal system, one for the somatic system and one for the whole *C. elegans* neural network. I started from a previous work made by a former MSc student (Cao, 2017; github.com/zaleCao/elegansNet). Models were built at the cellular level using Python 3.7.3 and Networkx 2.2 module. I created a graph with a node per neuron and directed edges per structural connections. Attributes with relevant properties were added to each node (cell name, cell type, cell 3D position, inhibitory/excitatory and if sensory: sensor type and location) and to each edge (connection type and weight).

First, among these properties added as attributes, characterization of inhibitory and excitatory neurons is based on each neuron's predominant neurotransmitters used (Loer & Rand, 2016; Pereira et al., 2015; Perrone, Sullivan, Pratt, & Margaryan, 2004; table 1).

Table 1. Excitatory/Inhibitory by neurotransmitter.

Acetylcholine (Ach)	Excitatory
Dopamine (DA)	
Serotonin (5HT)	
Glutamate (Glu)	
Octopamine (OT)	
Tyramine (Ty)	
GABA	Inhibitory
Unknown	Excitatory

Second, for sensory neurons, I specified the type of sensor (i.e. chemosensor, mechanosensory, odorsensor, etc.) and the location in the body (i.e. head, body and tail; right and left hemisphere). This information is used to start the simulations with sensory activation (random and/or specific) and to maintain a cyclical random sensory input during simulations, compartmentalized by sensor type and location. This compartmentalization means that when the sensor activation algorithm is executed (explained below), 40% of sensor types will be activated, out of those, 60% of location subgroups and, out of those, 80% of neurons. This way sensory activation tends to belong to the same sensor types and locations subgroups, trying to generate a somehow coherent sensory input to the virtual worm.

Third, the connection weights are based on the amount of Electron Microscopy slices where synapses between two neurons were found in Jarrell et al. (2012). This is a measure of synaptic size and number of synapses between each pair of neurons. Those weights are translated in our simulator to depolarization voltages. To our knowledge, literature on the relationship between synaptic size and postsynaptic depolarization is scarce and contradictory (Atwood & Karunanithi, 2002; Branco, Marra, & Staras, 2010). Most connections in the structural network had an original weight of 1 and some of them reached 80 (Fig.

1). Using these values linearly would mean that the latter connection generates 80 times the depolarization that most of neurons generate. I thought that the relationship should be positive but not linear. Thus, I applied a natural logarithmic transformation reducing the strong positive kurtosis in the distribution.

Lastly, connection types are used to differentiate between electrical synapses where activation is transmitted instantaneously, and chemical synapses where activation transmission has slight delay (Siegelbaum & Kandel, 2013).

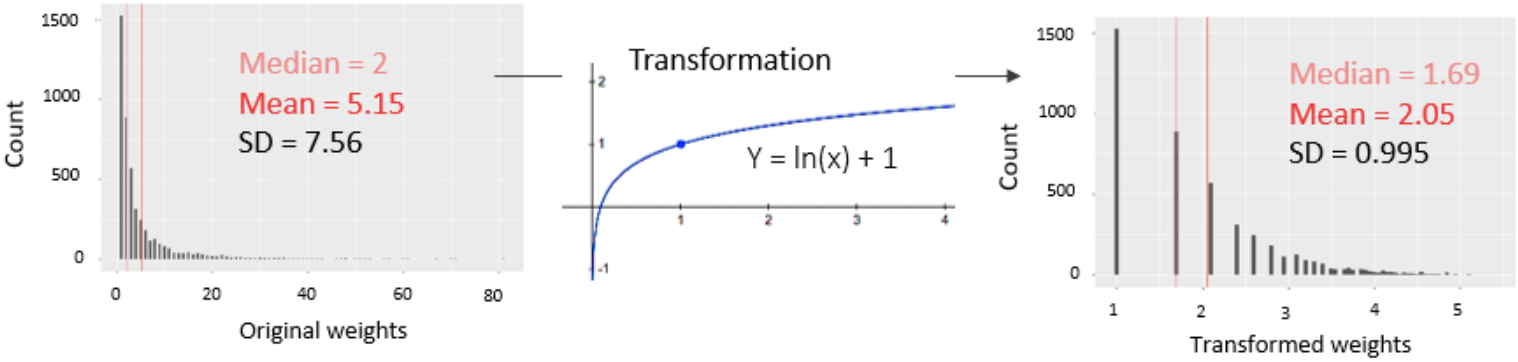

Figure 1. Weight transformation. Left, original weights from Jarrell et al. (2012). Middle, logistic transformation function. Right, final weights outcome with corrected kurtosis.

With this information we can build a model for our network. Our simulator implements an integrate and fire model of a neuron with resting potential at -70mV, threshold at -60mV, potential peak at -30mV and one timestep of absolute refractory period. It also implements a period of four timesteps (a cycle) of attenuation meant to be a mechanism of homeostatic plasticity in the network. Thus, a neuron that was activated the last cycle will have a reduction to its neighbours' chemical synaptic inputs exponentially related to the number of consecutive cyclic activations. It mainly affects chemical synapses as the cellular mechanisms of homeostatic plasticity expression are based on neurotransmitter release and postsynaptic receptors (Pozo & Goda, 2010).

There are four parameters we can specify in our model. Random initial activity (*RI*) determines the proportion of sensory cells randomly activated at the beginning of the simulation. Synaptic efficacy coefficient (*c*) multiplies connection weights mediating the amount of depolarization transmitted through

a synapse. Attenuation coefficient (*att*), is a value between 0 and 1 that implements homeostatic adaptation to the network's activity reducing inputs as a neuron is consecutively activated (Eqs. 1 and 2). Finally, we have *Psens* (probability of sensory stimulation) that determines the probability of sensor stimulation during the simulation. The integrated input into a neuron at a given timestep is computed as follows

Eq. 1 $\mathrm{I} = \sum_{k=1}^{n} 30 * w * sgn * c * att^{ca}$; for chemical synapses

Eq. 2 $\mathrm{I} = \sum_{k=1}^{n} 30 * w * sgn * c * att$; for electrical synapses.

Where *I* stands for integral, *n* for number of a neuron's neighbours, w for structural weight, *sgn* for inhibitory (-1) or excitatory (+1) connection, *c* for synaptic efficacy, *att* for attenuation coefficient and *ca* for consecutive activations. The constant '30' is a superfluous value inherited from previous models that could be removed in future versions of the simulator.

To represent activity patterns, I used 2D and 3D representations. 2D representations were achieved within Networkx module, plotting node degree by size and activity by colour (Fig. 2a). 3D representations were achieved with Plotly 3.6.0 module implementing cell positions into a 3D space, and colour coding activity and cell type (Fig. 2b).

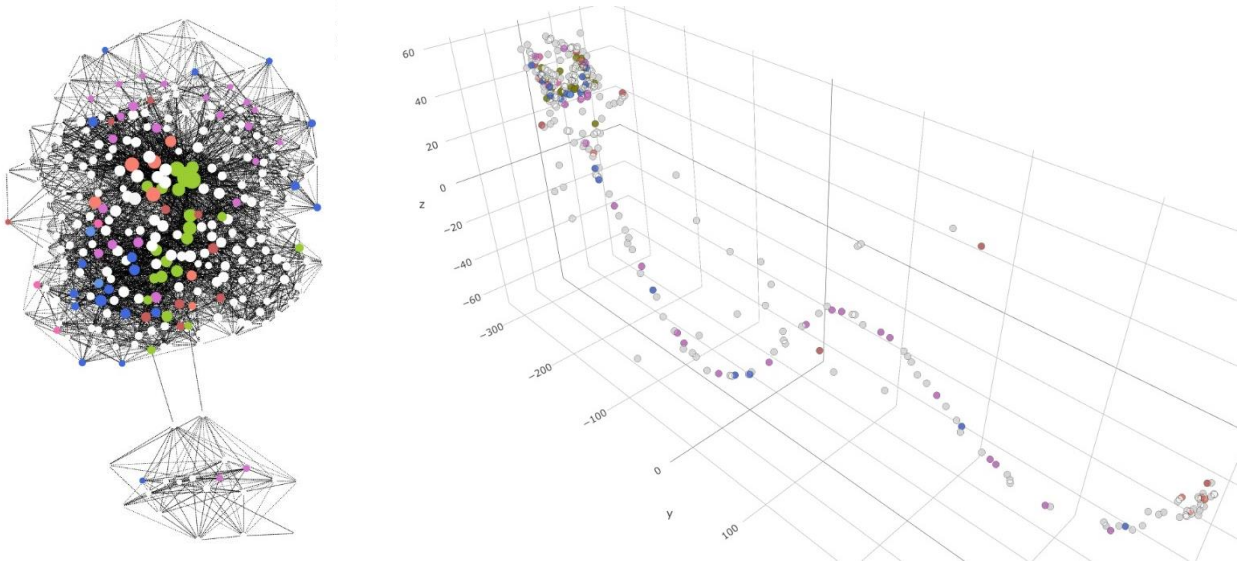

Figure 2. 2D (left) and 3D (right) representations. Circles as nodes. Colour coded active nodes by cell type. Reds (sensors-interneuron) to greens (sensory-motors-interneuron) to blues (motor-interneurons). Grey scale for non-active nodes.

Out of the three simulators developed, I used the whole *C. elegans* neural network to validate the network's activity compared to electrophysiological recordings (parameters: *RI* = 0.3, *c* = 0.2, *att* = 0.7, *Psens* = 0.2). Pharyngeal and somatic systems were used to carry out structural-functional explorations. This division allowed us to test analysis pipelines (i.e. network characterization and Granger Causality analysis) with a structurally simpler and computationally inexpensive pharyngeal system (20 neurons) and to deepen in the analysis and results. Once with pipelines tested and ready, I applied them to the more complex and complete somatic system of 279 neurons, after having removed three of them (CANL/R and VC06) that do not have any connections to other neurons following Varshney *et al.* (2011). The latter analysis lasted for around three weeks of parallelized computing.

Network Characterization

Before obtaining simulated activity for further analysis, I wanted to control simulators' behaviour and to be sure that network activity fulfilled some minimum criteria as: every node in the network must be able to be activated, activity might be able to be sustained until the end of a simulation, the implemented neural homeostatic adaptation doesn't impede neurons to reactivate consecutively, and we know approximately how many sensors will be activated during simulations. I analysed the influence of each of the implemented parameters over the operationalization of these minimum criteria (dependent variables). To do this, I simulated repeatedly activity in the network with different combinations of parameters measuring each of those variables.

To characterize Pharynx network activity, I used 50 simulations of 50 timesteps each per combination of parameters (344,250 simulations in total):

```
RI = [0.2,0.25,0.3,0.35,0.4];
c = [0.01,0.05,0.1,0.2,0.25,0.3,0.35,0.4,0.45,0.5,0.55,0.6,0.65,0.7,0.8,0.9,1];
att = [0.1,0.2,0.3,0.4,0.5,0.6,0.7,0.8,0.9];
Psens = [0.1,0.2,0.3,0.4,0.5,0.6,0.7,0.8,0.9].
```

To characterize Somatic network activity, I used 100 simulations of 50 timesteps each per combination of parameters (160,000 simulations in total):

```
RI = [0.1,0.2,0.3,0.4,0.5];

c = [0.01,0.05,0.1,0.15,0.2,0.25,0.3,0.35,0.37,0.39,0.41,0.43,0.45,0.5,0.6,0.7];

att = [0.2,0.4,0.6,0.8,0.9];

Psens = [0.2,0.4,0.6,0.8].
```

Once with control over the simulators, I generated activity to apply Ganger Causality. For pharynx, I gathered 100,000 timesteps of network activity simulation (parameters: *RI* = 0.4, *c* = 0.5, *att* = 0.5, *Psens* = 0.5), for somatic, 50,000 timesteps (parameters: *RI* = 0.4, *c* = 0.38, *att* = 0.3, *Psens* = 0.5).

Granger Causality Analysis

To extract the functional connectivity network from simulated activity, I used MATLAB R2018a implementing an algorithm designed and coded by Kim, Putrino, Ghosh, & Brown (2011). It executes a Granger Causality analysis over Point Process models fitted to predict spiking of a single target neuron.

A point process is a sequence of discrete events that happen in a time space. Neural activity can be viewed from this perspective. Point process modelling consists in fitting generalized linear models (logistic regression; Eq. 3) with a parameter per trigger neuron and per timestep of history to calculate the likelihood of a target neuron's activation in a specific timepoint (alternative models, M_1). The algorithm generates several models with different history time extensions to compare between their throughput with Akaike criterion, choosing the optimal one. I calculated 10 different history time extensions ranging from 2 to 20 timesteps of history. Each of these models offer a measure of target neuron activation's likelihood as a function of other neurons' activity history.

$$Eq.3 \qquad logit(y) = \beta_0 + \beta_1 x_1 + \beta_2 x_2 + \beta_3 x_3 + \beta_4 x_4 + \beta_5 x_5 + \cdots + \beta_p x_p$$

After defining the optimal generalized linear models, Granger Causality analysis calculates the relative reduction in likelihood between those optimal models -that consider every neurons' influence (alternative models, M_1)- and models that doesn't consider the parameters of one potential trigger neuron (null model, M_0). Null models propose that a trigger neuron doesn't have a significant influence on a target neuron so we could remove its parameters from the model and still have the same accuracy in the predictions. For each connection, we will compare these two models, if null model is rejected, we could say that the connection is statistically significant.

To calculate this statistical significance, the algorithm uses deviance and likelihood ratio. Deviance (D) is a measure of the amount of error that each proposed model generates in the predictions of a target neuron's activation. If a saturated model (M_s) is the one having a parameter per data point and, therefore, predicting without error, deviance is defined as D = -2 (Log Likelihood M – Log Likelihood M_s) where M is any model proposed. Likelihood ratio (G_{0-1}) serves to test the statistical significance of the reduction in deviance between two proposed models (i.e. H_0: $\theta = M_0$, H_1: $\theta = M_1$). It is calculated as $G_{0-1} = D_0 - D_1$ and its probability distribution follows a Chi-squared. Therefore, if M_0 error (D_0) differ from M_1 error (D_1) in a value over the critical point of the distribution, then the connection is considered statistically significant and we would reject H_0.

The analysis for somatic system (279 neurons) takes around 4000 hours to be carried out. In order to optimize temporal resources, I parallelized the analysis and executed it in the Edinburgh Compute and Data Facility cluster (EDDIE).

Data analysis and visualization

I used R 3.6 and ggplot2 3.2.0 to analyse and visualize results. This includes characterization of simulated network dynamics and comparisons between structural and functional networks. Codes for this part and the previous two can be found in github.com/jescab01/elegansProject.

Results

Simulator validation

Our **second aim** - after developing the simulator - was to obtain a validation proof for our model. It came from the similarity of its activity dynamics (using *C. elegans* whole network represented in 2D and 3D; Fig. 3A), and the activity dynamics observed in a set of calcium imaging recordings from *C. elegans* nervous system (Nguyen et al., 2016) shown frame by frame (Fig. 3B).

Our simulator shows an oscillatory pattern of activation with wavelength of 4 timesteps. In this cycle, the first step shows the largest amount of activation and it decreases progressively towards the fourth timestep. In our model, this cyclical activity is a consequence of the implementation of chemical synaptic delay equal to 3 timesteps.

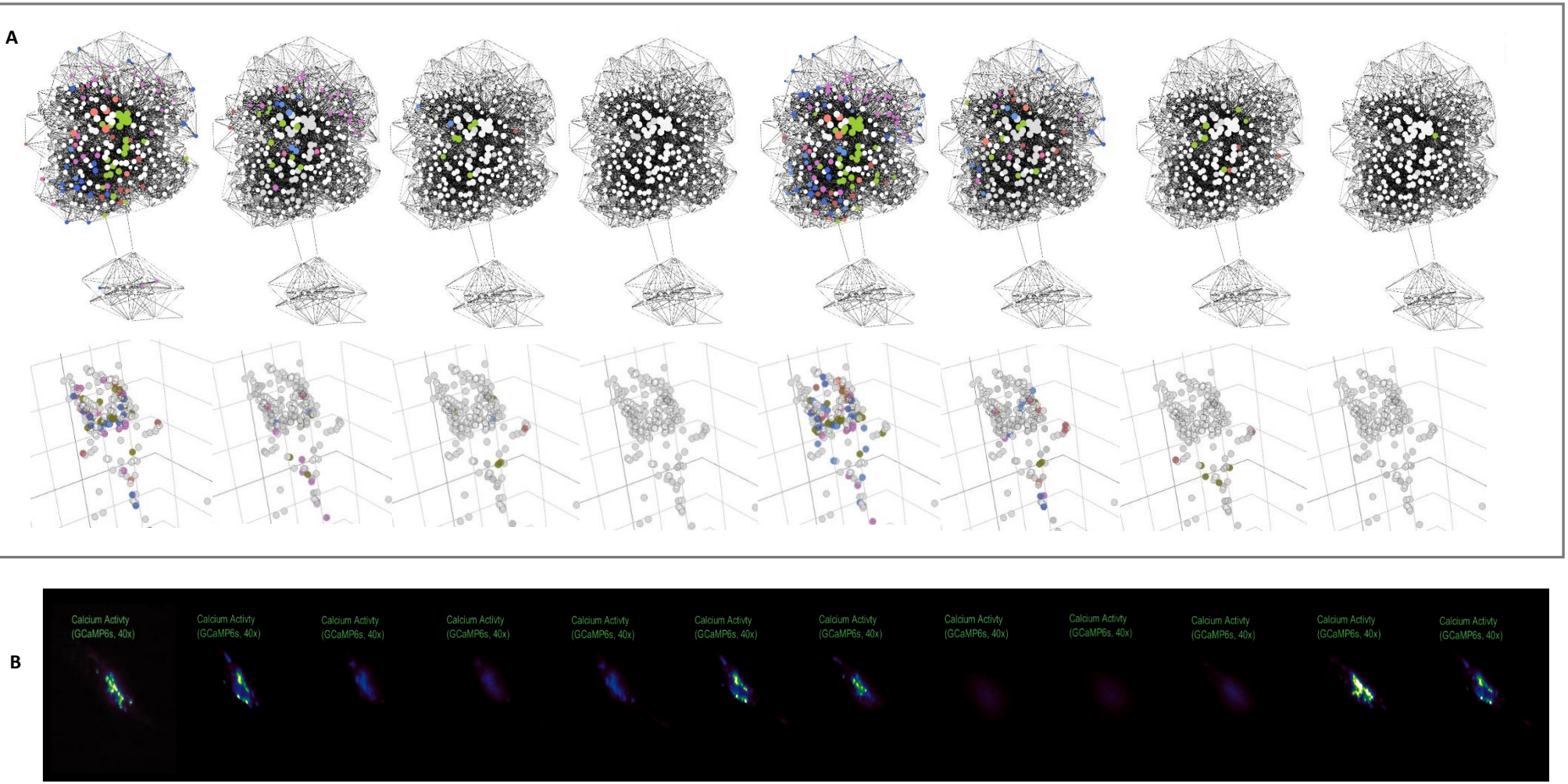

Figure 3. Activity dynamics validation. A) Two cycles of simulated activity represented in 2D and 3D colour coding by activity and neuron type. Reds for active sensory-interneurons, greens for active sensory-motor, blues for active motor-interneurons. Grey scale for non-active nodes. Showing just head in 3D representation. Timesteps per frame shown in sequence. Videos available on Stefan lab channel (YouTube). B) Calcium imaging recordings adapted from Nguyen et al. (2016) showed frame by frame (each frame represents 33ms).

Electrophysiological recordings taken from *C. elegans* head also show an oscillatory pattern of activation with a wavelength of about 166 ms. The activation decreases gradually from a point of maximum activation to a point of no activation, raising again eventually to repeat the pattern.

The colour coding in our representations distinguished by activated cell types. I wondered if there were any pattern in the sequential activation of cell types. For instance, I checked if our model's cycles represented a flow of information from sensory neurons to motor neurons, but this was not the case. I didn't find any pattern in the dynamics of specific neuron types.

I am aware of the weakness of this proof of validation, nevertheless for the purposes of this research - relationship between structural and functional neural networks- having this similar pattern of activity is enough.

Network activity characterization

Our simulators implement several parameters (synaptic efficacy (*c*), attenuation coefficient (*att*), probability of sensor stimulation (*Psens*), random initial activation (*RI*)) defining aspects that are not theoretically clear: relationship between structural weights and postsynaptic depolarization, temporal dynamics of environmental sensory inputs and the temporal dynamics of neural homeostatic adaptation. Therefore, I wanted to characterize their influence - **third aim** - on several aspects of network activity that could generate an interaction with the following Granger Causality analysis. I characterized network activity for: persistence, minimum node activity, attenuated potentials and sensory stimulation.

Persistence

I wanted to know how parameters affect temporal dynamics of network activity in terms of persistence (i.e. Is there activity in the network at the end of simulation time?). Thus, dependent variable was dichotomic with values: 1 if network's activity lasted until the end of simulation (50 timesteps); 0 if network activity was null before reaching the end. I fitted a logistic regression model to analyse the influence of each parameter on this dependent variable.

For pharyngeal system, synaptic efficacy was the best predictor B = 11.08, SD = 0.038, $p < 2x10^{-16}$, followed by random initial activity B = 6.737, SD = 0.0792, $p < 2x10^{-16}$. Attenuation coefficient B = 0.217, SD = 0.021,

$p < 2x10^{-16}$ and probability of sensory stimulation B = 0.94, SD = 0.02, $p < 2x10^{-16}$, although having positive coefficients and statistically significant influences, their effect sizes were small.

For the somatic system, synaptic efficacy was again the best predictor with B = 36.36, SD = 0.294, $p < 2x10^{-16}$. Surprisingly, probability of sensory stimulation was the second most important variable B = 8.466, SD = 0.087, $p < 2x10^{-16}$ over random initial activity B = 3.574, SD = 0.099, $p < 2x10^{-16}$. This difference could be due to the larger number of sensors in somatic network combined with a fixed probability of stimulation per sensor in simulation's algorithms. This will result in more sensors activation during simulations in somatic system and its consequent effect on maintaining activity in the network. Attenuation coefficient influence was again small B = 0.394, SD = 0.0531, $p = 8.68x10^{-14}$.

These results show the consistent relevance of synaptic efficacy in driving the amount of network activity. Also, that this influence is supported differentially by random initial activation for pharynx and by probability of sensor stimulation for somatic system.

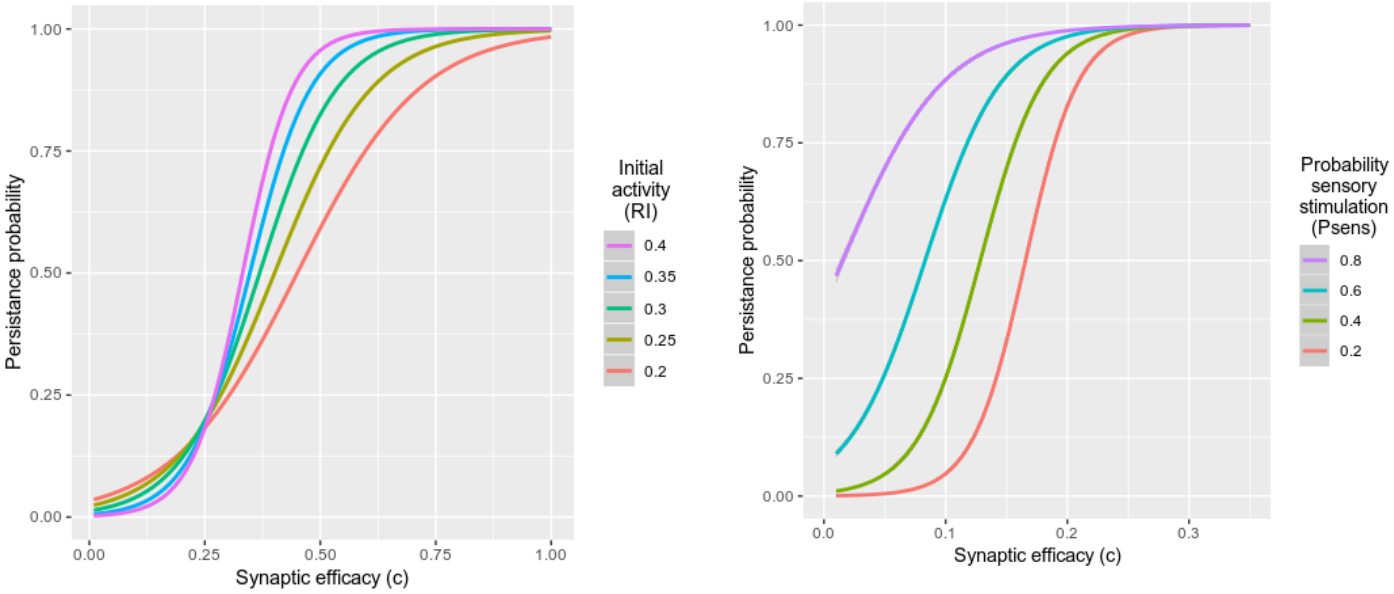

Figure 4. Characterization of network persistence. Left, pharynx system, colour coding the percentage of sensors activated at the beginning of the simulation. Right, somatic system, colour coding the probability of sensor stimulation.

Minimum node activity

From now on, I will focus on persistent simulations (i.e. simulations whose activity lasted until the end). Minimum node activity refers to the number of potentials that the node with less activity at the end of each simulation had. This dependent variable let us control if every neuron in the network can reach threshold and be activated with specific sets of parameters. Neurons with low weights and few connections could be at risk of being unable to participate in the activity dynamics within our simulator. I fitted a Poisson regression model to analyse dependent variable's count data.

For pharynx, the most important influence was synaptic efficacy B = 2.319, SD = 0.00499, $p < 2x10^{-16}$, followed by attenuation coefficient B = 1.123, SD = 0.0048, $p < 2x10^{-16}$, random initial activity B = 0.942, SD = 0.0146, $p < 2x10^{-16}$, and probability of sensor stimulation B = 0.023, SD = 0.00395, $p = 6.06x10^{-9}$.

The somatic system repeats the relative pattern as in persistence. First variable was synaptic efficacy B=9.333, SD=0.025, $p<2x10^{-16}$, followed by probability of sensor stimulation B = 1.46, SD = 0.015, $p < 2x10^{-16}$ consistent with results in persistence, attenuation coefficient B = 0.725, SD = 0.013, $p < 2x10^{-16}$ and random initial activation B = 0.52, SD = 0.021, $p < 2x10^{-16}$.

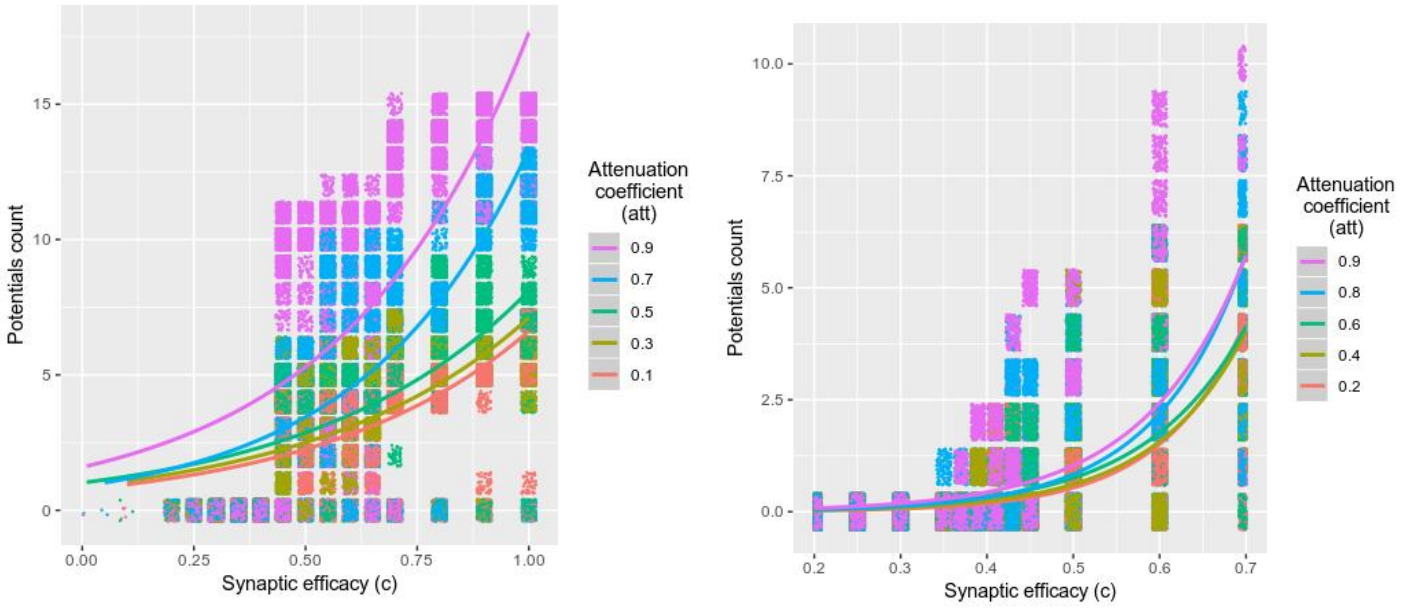

Figure 5. Minimum node activity characterization. Each dot as a simulation and Poisson's regression curves fitted to the data. Colour coding attenuation coefficient.

As minimum node activity explores the activity of less connected neurons, these results suggest that attenuation coefficient has relative relevant impact on less connected neurons' reactivation in subsequent cycles. It is synaptic efficacy parameter what determines if an isolated neuron will be able to have a potential or not ($c > 0.4$ in Pharynx, $c > 0.3$ in somatic) but once over this threshold attenuation coefficient will determine the amount of activation for those cells. When simulating activity for further analysis, I chose synaptic coefficient values over those values (c = 0.5 in pharynx, c = 0.38 in somatic system).

Attenuated potentials

This refers to the number of activations occurred during attenuation period (i.e. period of 4 timesteps after a neuron has been activated). As a neuron is consecutively activated its inputs will be reduced in intensity being multiplied by *att* for electrical synapses and by att^{ca} for chemical synapses, where "*att*" is a parameter between 0 and 1 and "ca" refers to number of consecutive activations. This structure allows the network to control its activity (homeostatic adaptation) when it is overactivated. I wanted to know what variables influence this phenomenon and what is the proportion of attenuated spikes as a function of those variables. Does that proportion plateau with some combination of parameters? Is there a minimum of attenuation coefficient to allow neurons to fire consecutively?

This variable was mainly predicted by attenuation coefficient B = 3.149, SD = 0.0016, $p < 2x10^{-16}$ (pharynx), B = 3.61, SD = 0.0006, $p < 2x10^{-16}$ (somatic) and synaptic efficacy B = 1.596, SD = 0.002, $p < 2x10^{-16}$ (pharynx), B = 3.85, SD = 0.0012, $p < 2x10^{-16}$ (somatic). Random initial activation B = -0.13, SD = 0.006, $p < 2x10^{-16}$ (pharynx), B = -0.33, SD = 0.001, $p < 2x10^{-16}$ (somatic) and probability of sensor stimulation coefficient B = 0.09, SD = 0.0016, $p < 2x10^{-16}$ (pharynx), B = -0.02, SD = 0.0007, $p < 2x10^{-16}$ (somatic) showed small effect sizes.

Figure 6 shows how high attenuation coefficient and high synaptic efficacy parameters raise over 90% the proportion of attenuated potentials in a simulation. This means almost every activated neuron will re-activate cyclically. This combination would generate static network activity patterns repeated cyclically over the whole simulation where every neuron is activated at the same cycle point. It is a situation to avoid for further Granger Causality analysis as richness in network activity will impact the richness of connectivity predictions.

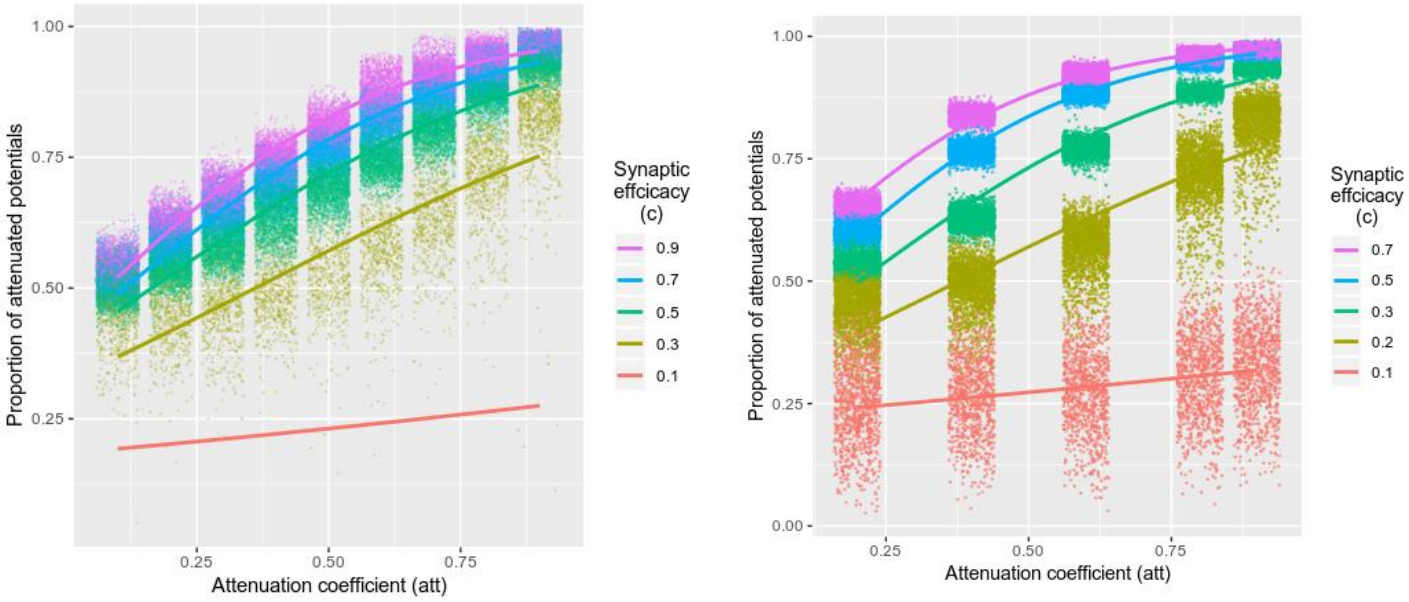

Figure 6. Attenuated potentials. Each dot as a simulation and Poisson's curves fitted. Colour coded by synaptic efficacy.

Sensory stimulation

This variable is fully controlled by *Psens* parameter in our algorithm. It calculates random activation for sensors during a simulation, compartmentalizes cells into sensor type groups and cell location subgroups (Fig. 7). This way, we achieve a more coherent sensory stimulation with several sensors of the same type in the same location being activated at the same time. This algorithm is executed each 4 timesteps with *Psens* probability. Once the algorithm is executed it gives a probability P = 0.3 in pharynx and P = 0.4 in somatic to each sensor type group, P = 0.6 to each location subgroup and P = 0.8 to each neuron. I wanted to know how *Psens* parameter affects the number of groups, subgroups and neurons eventually being stimulated.

The number of times the algorithm is executed in a simulation depends directly on *Psens* value for both pharyngeal and somatic systems: NE = *Psens* x timesteps/4 = *Psens* x Cycles, where NE stands for number of executions. The average number of groups, subgroups and neurons activated per simulation are shown

in figure 8A (pharynx) and figure 8B (somatic). The raising averages from group to neurons with the same *Psens* shows that the algorithm is capable of stimulation compartmentalization, giving a more coherent sensory input to the network.

```
sensWhole={'chemosensor':{'headL':['n4','n6','n39','n41','n43','n45','n47','n49','n123'],
                          'tailL':['n139','n141'],
                          'headR':['n5','n7','n40','n42','n44','n46','n48','n50','n124'],
                          'tailR':['n140','n142']},
           'odorsensor':{'headL':['n72','n74','n43','n76'], 'headR':['n73','n75','n44','n77']},
           'oxygen': {'headL':['n78','n232'], 'headR':['n27','n79','n233'],
                      'tailR':['n149']},
           'nociceptor':{'head':['n43','n44']},
           'osmoceptor':{'head':['n43','n44']},
           'thermosensor':{'head':['n8','n9','n76','n77'],'body':['n152','n153','n111','n112']},
           'mechanosensor':{'body':['n71','n154','n23','n137','n24'],
                            'body1':['n138','n152','n153','n111','n112'],
                            'headL':['n2','n82','n84','n117','n129','n131','n133','n43'],
                            'headR':['n3','n83','n85','n118','n130','n132','n134','n44'],
                            'tail':['n145','n146']},
           'propioSomatic':{'body':['n86','n87','n88','n89','n90','n91','n92','n93','n94','n95'],
                            'body1':['n96','n97','n98','n99','n100','n101','n238','n239','n240'],
                            'body2':['n241','n242','n243','n244','n245','n246','n247','n248'],
                            'body3':['n249','n250','n251','n252','n253','n254','n255','n256'],
                            'body4':['n257','n258','n259','n260','n152','n153','n111','n112'],
                            'tail':['n108','n150','n151', 'n147','n148']},
           'propioHead':{'L':['n201','n203','n218','n220','n222','n224'],
                         'R':['n202','n204','n219','n221','n223','n225']},
           'propioTail':{'tail':['n63','n136','n161','n145','n146', 'n147','n148']},
           'propioPharynx':{'L':['n281','n283','n292','n296','n299'],
                            'R':['n282','n284','n293','n297','n300'],
                            'b':['n285','n287','n288']}}
```

Figure 7. Sensor type groups, location subgroups and nodes implemented in the simulator. In Networkx module cells are named with numbers as shown.

A

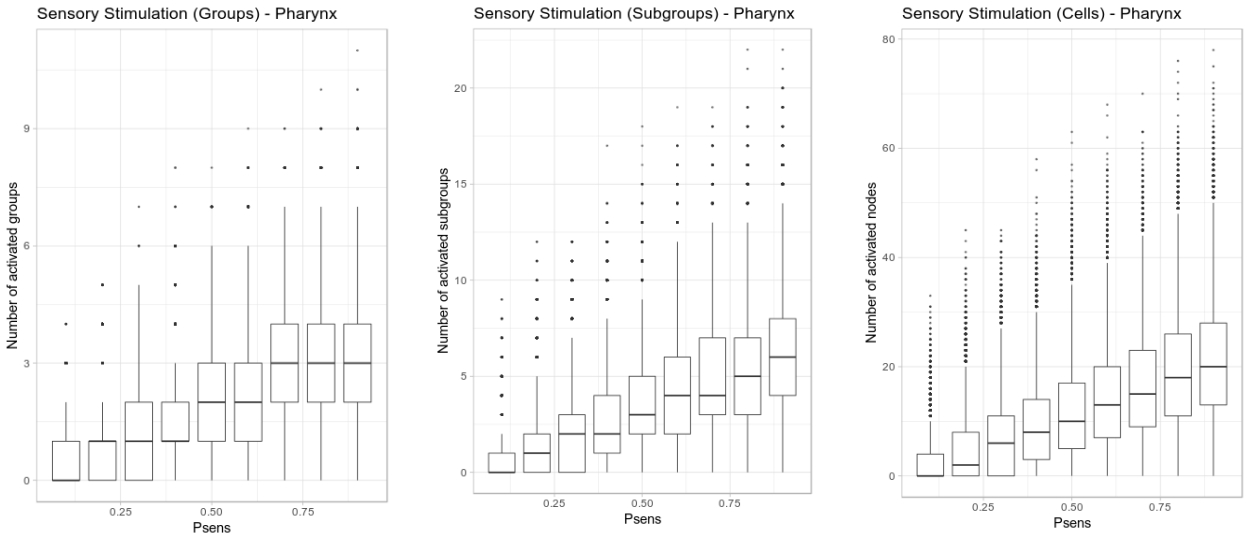

Figure 8a. Number of cell type groups, location subgroups and cells activated per simulation in Pharyngeal system.

B

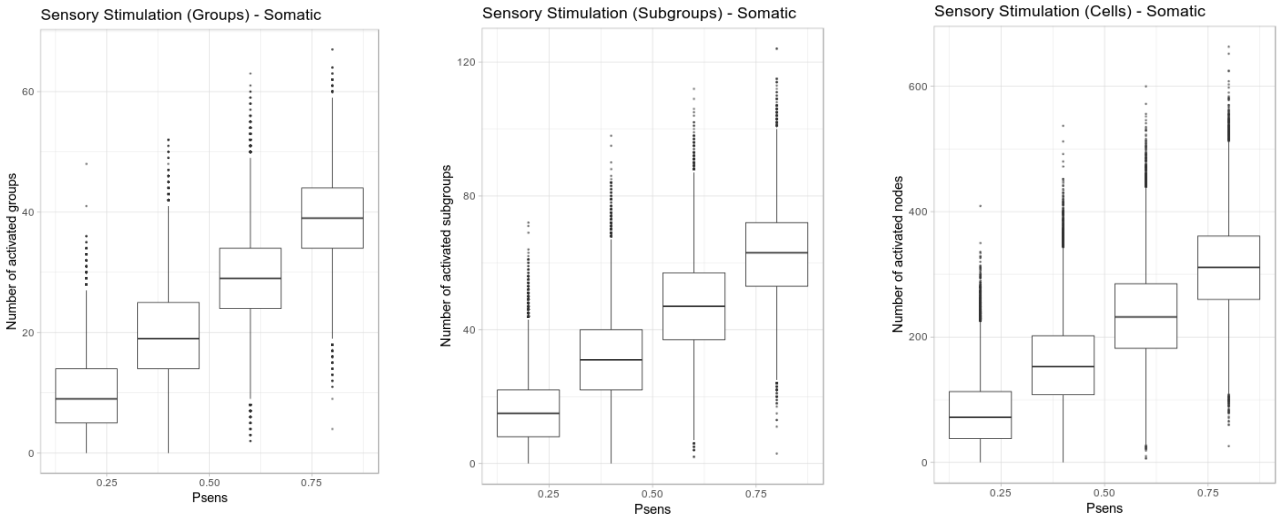

Figure 8b. Number of cell type groups, location subgroups and cells activated per simulation in Somatic system.

I used all this characterization to choose a set of parameters that allow us to obtain a rich pattern of activity dynamics. As stated in methodology, for pharynx I used *RI* = 0.4, *c* = 0.5, *att* = 0.5, *Psens* = 0.5, and for somatic, *RI* = 0.4, *c* = 0.38, *att* = 0.3, *Psens* = 0.5.

Granger Causality analysis

After gathering activity - **fourth aim** - and applying Granger Causality analysis – **fifth and sixth aims** -, the first phenomenon I noticed in our results were strong anticorrelations for neural self-connections consistent through pharyngeal and somatic systems (Fig. 9). I explain this first, because I considered it not directly informative and a source of error for further analysis, so I decided to exclude self-connectivity from the analysis.

This result could be due to an interaction between our models, implementing absolute refractory period, and Granger Causality analysis' pipelines considering for every prediction the timestep before the predicted potential. On the other hand, attenuation period could also be supporting this phenomenon as the consecutive activation of a chemical synapse in our model suffer a process of homeostatic adaptation. This means for self-connections that the more consecutive activations they have the less probability to activate again, contributing to the anticorrelation observed.

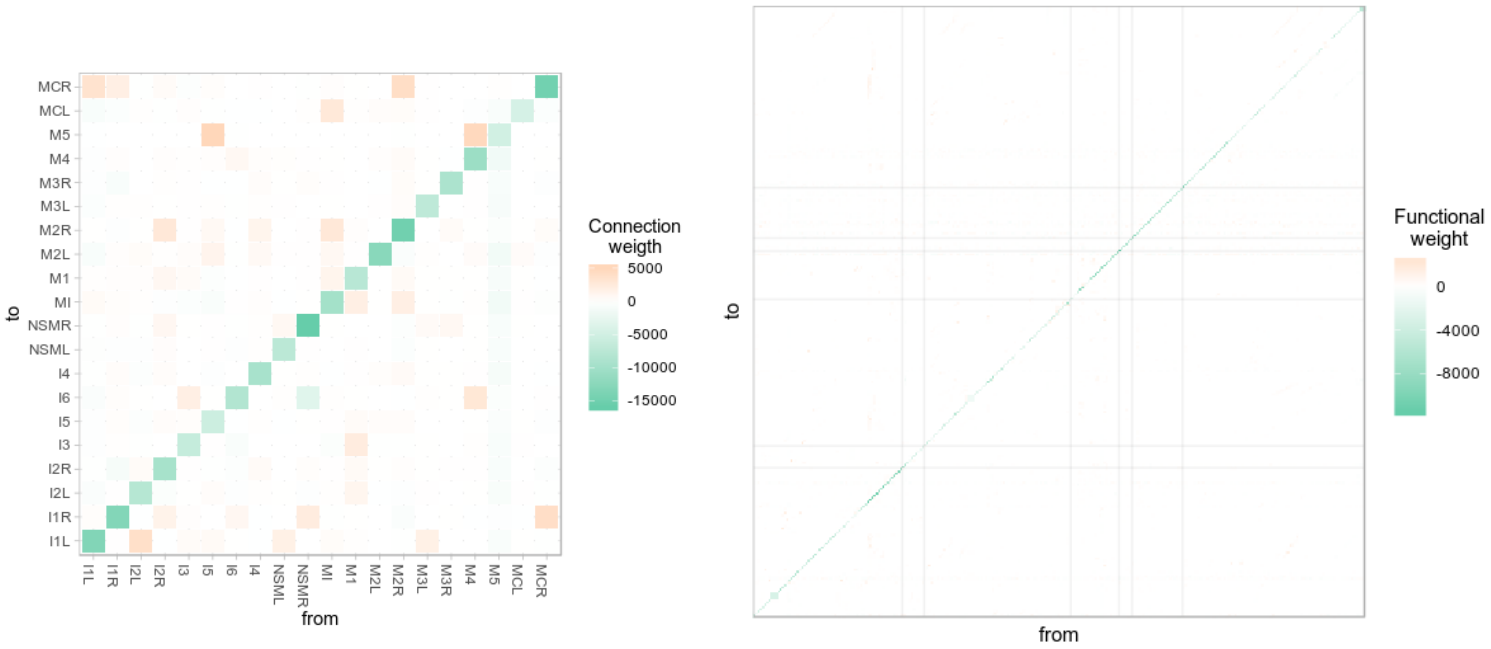

Figure 9. Pharyngeal (left) and Somatic (right) original functional connectivity matrices showing strong anticorrelation in self connections.

Therefore, I will focus below on *between* neurons connectivity, tackling **aims seventh and eighth**.

Pharynx analysis

Pharyngeal nervous system has 20 neurons: 7 sensory-interneurons (35%), 1 Interneuron (5%), 2 motor-sensory (10%), 1 motor-interneuron (5%) and 9 motor (45%). They are connected by 128 chemical synapses and 64 electrical synapses, all of them excitatory (Fig. 10).

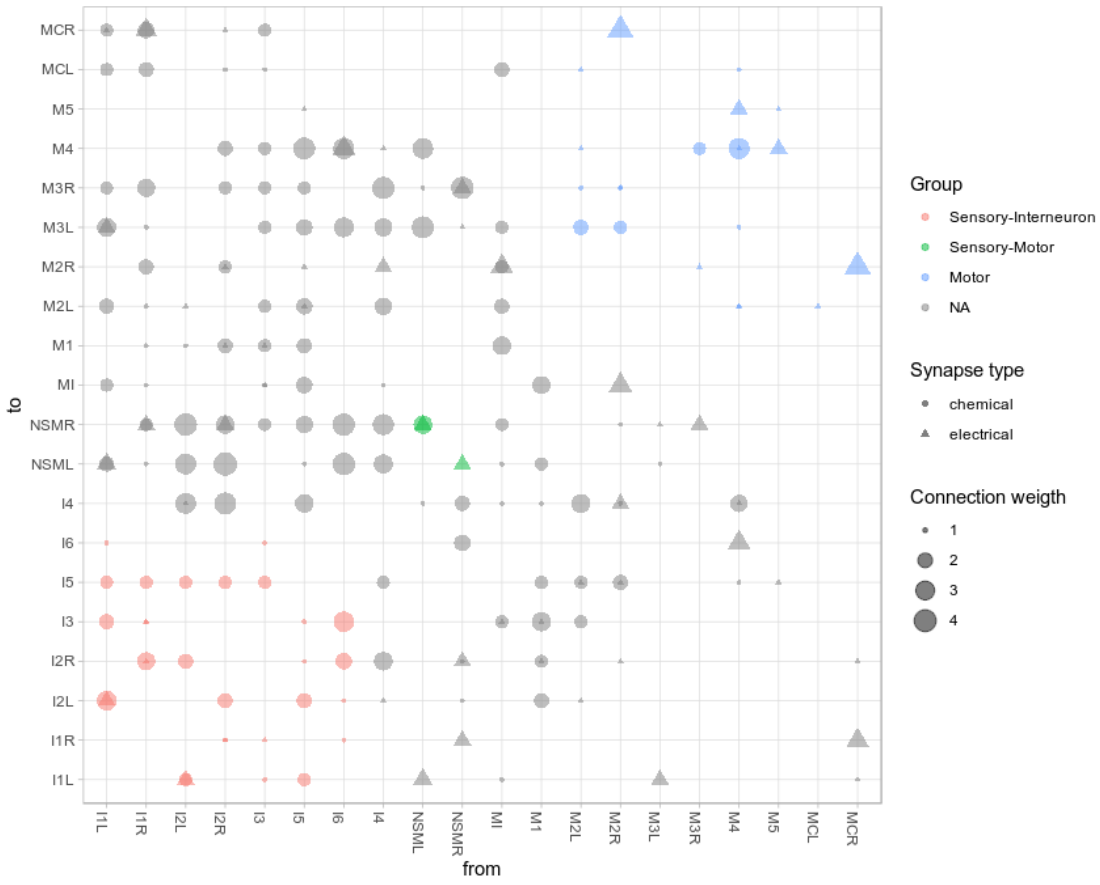

Figure 10. Pharynx nervous system structural connectivity arranged by cell types. Each colour group represents the connections between neurons of the same type. Directed connectivity matrix.

After removing self-connections, we have a clearer picture of connectivity between neurons (Fig. 11). Most functional predicted connections show a positive weight (i.e. trigger neuron use to be activated before target neuron activates) consistent with the fact that structural connectivity in pharynx is just excitatory. For neuron M5, it is predicted an anticorrelation towards almost every other neuron. This could be due to its isolation in this network (it connects with just two neurons).

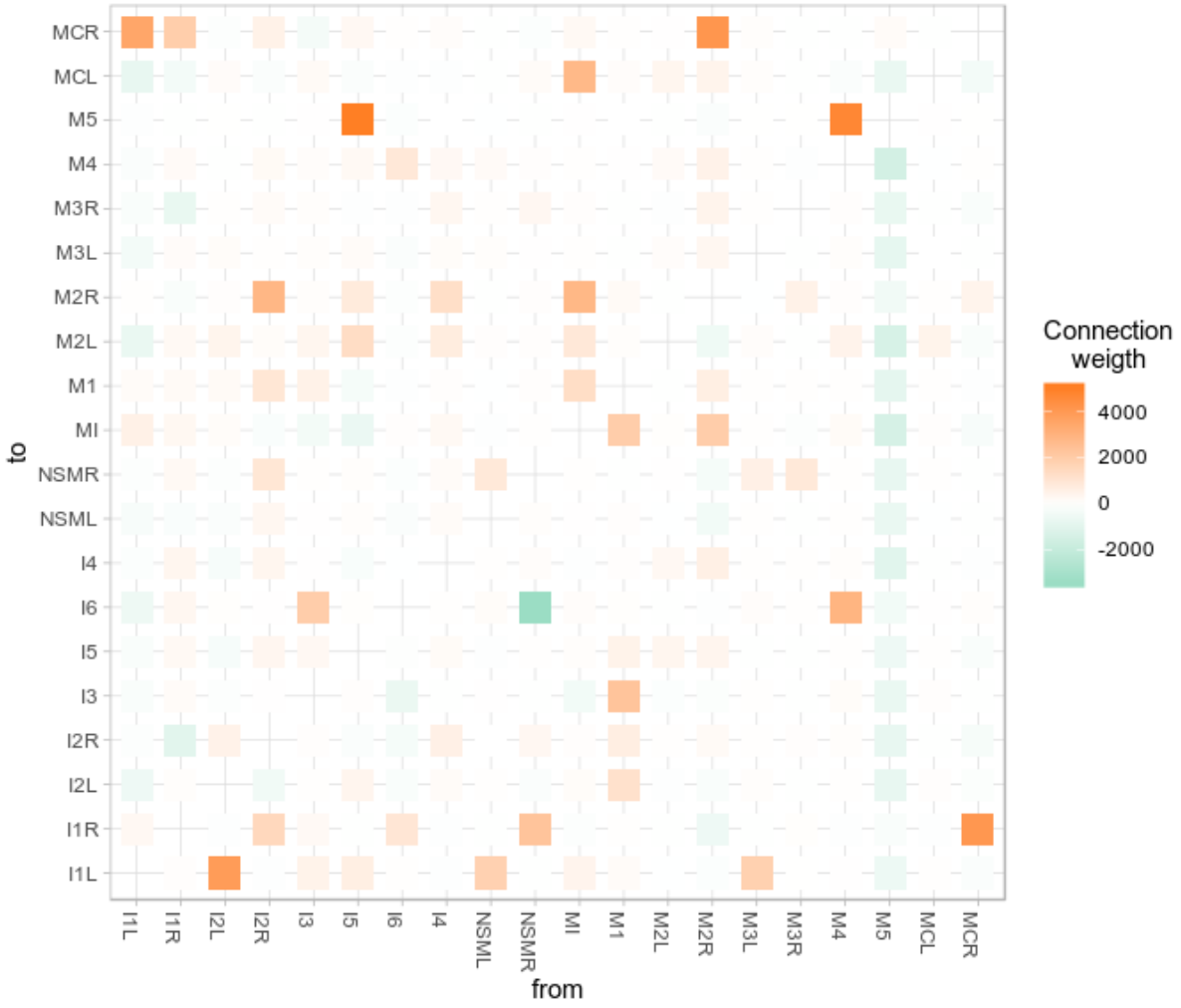

Figure 11. Functional connectivity matrix pharynx.

In pharynx, I first tested Granger Causality analysis predictions of the existence of excitatory connections (Table 2) showing sensitivity = 0.7025 and specificity = 0.5. I also calculated categorical correlation with a Chi-squared test which was statistically significant with Chi-squared = 16.791, df = 2, $p = 1.83 \times 10^{-5}$. This supports our second hypothesis that there is a categorical correlation between the existence of connections in structural and functional networks. These results support our **second hypothesis** for pharynx system.

Table 2. Adjacency matrix for structural – functional connections in pharynx system.

		Structural connections		
		Excitatory	*Non-Existent*	*Total*
Functional connections	*Positive r*	111	111	222
	Null	0	3	3
	Negative r	47	108	155
	Total	158	222	380

Second, I tested the correlation between structural and functional weights with a Pearson's correlation test over the 111 true positive cases (i.e. structural excitatory and functional positive correlation). The result was a positive correlation but not statistically significant r = 0.151, 95% CI = [-0.036, 0.329], t = 1.599, df = 109, p = 0.1125 (Fig. 12). Effect size was low. These results fail to support **our third hypothesis** for pharynx that structural and functional weights are positively correlated.

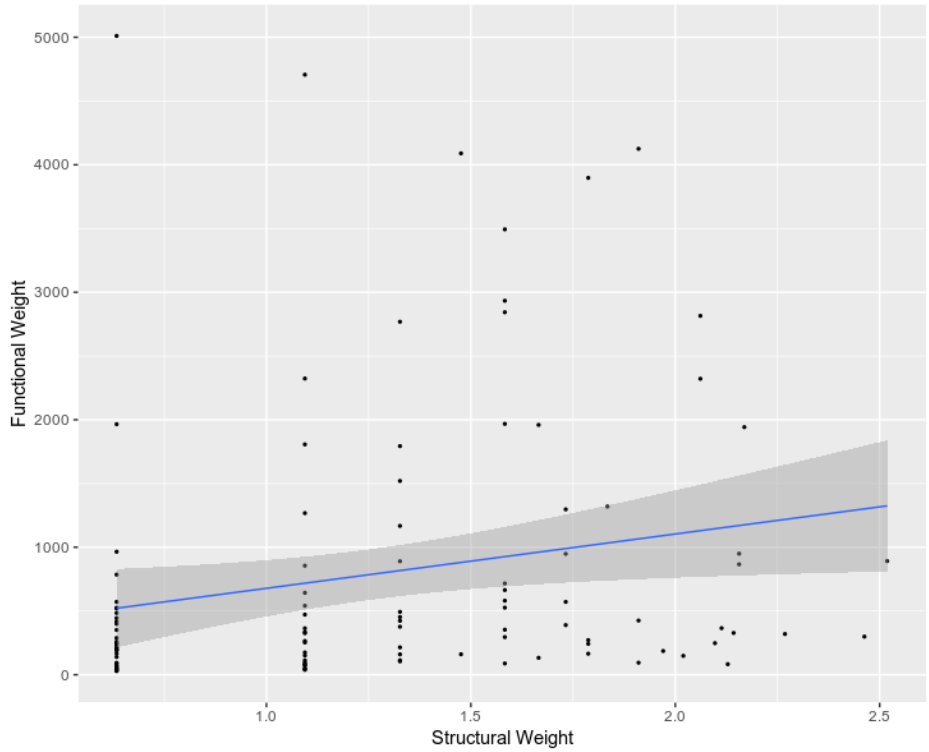

Figure 12. Correlation between structural and functional weights. Points as connections and a linear regression model fitting data.

Finally, examining carefully a merged structural-functional matrix (Fig. 13), I observed a possible higher correlation for electrical synapses' weights in front of chemical ones. Therefore, I decided to explore specific weight correlations for electrical and chemical synapses. Analyses supported the first impression: correlation with electrical weights was positive, moderate-high and statistically significant r = 0.37, 95% CI = [0.11, 0.59], t = 2.783, df = 48, p = 0.0077 but there was no correlation with chemical weights r = 0.024, 95% CI = [-0.189, 0.2362], t = 0.221, df = 83, p = 0.835.

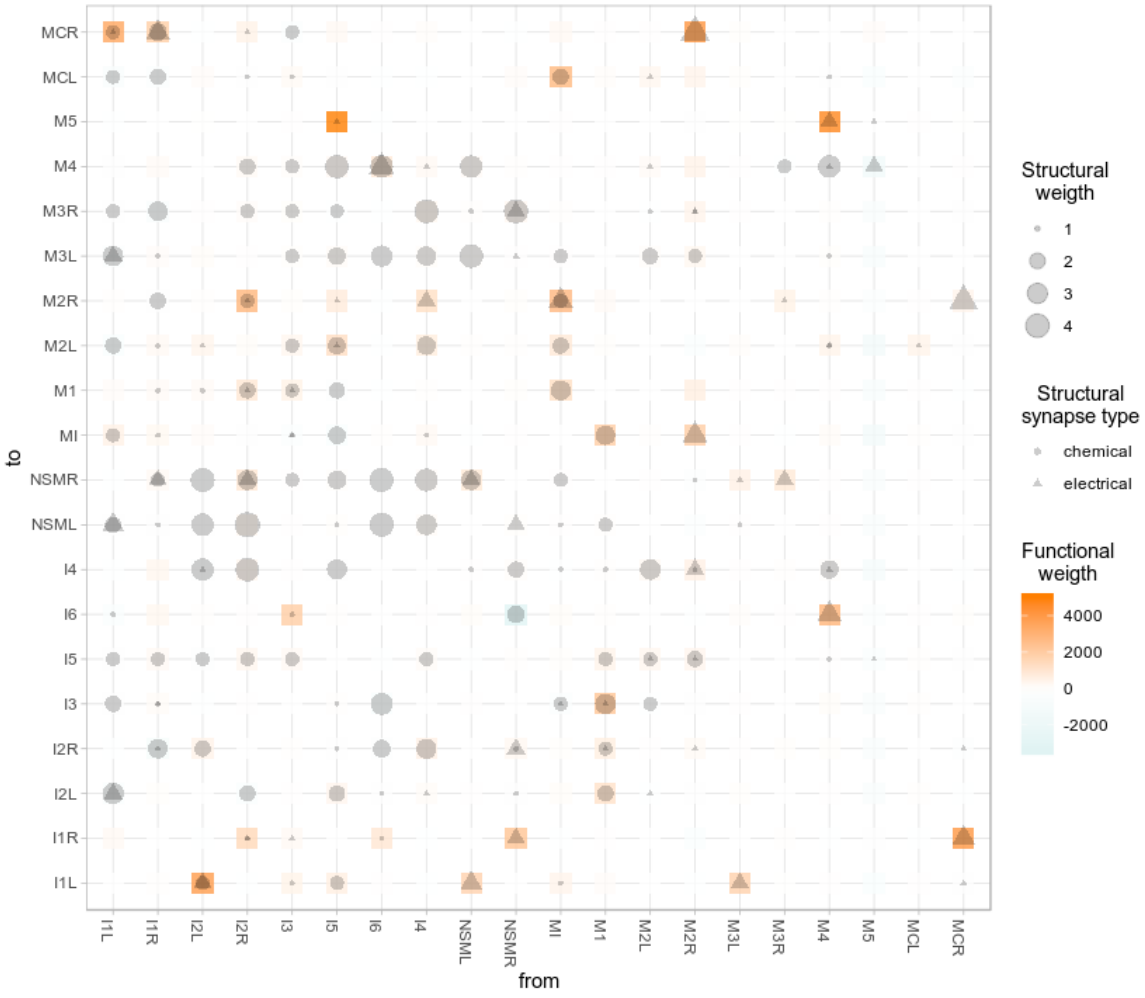

Figure 13. Merged structural functional matrix. Note that electrical synapses (triangles) seem to be more often present when there is a high functional weight (orange squares).

Following this analysis, I wanted to explore in the same way (differentiating electrical and chemical synapses) previous categorical predictions. Results showed significant categorical correlations for both electrical synapses (Chi-squared = 18.709, df = 2, p = 8.66×10^{-5}) and chemical synapses (Chi-squared = 10.4, df = 2, p = 0.00552), the same measures for specificity (specificity = 0.5) and a difference of 0.13 in sensitivity (electrical synapses' sensitivity = 0.806; chemical synapses' sensitivity = 0.669).

Somatic analysis

Somatic nervous system has 279 neurons: 68 sensory (24.4%), 14 sensory-interneurons (5%), 63 Interneuron (22.5%), 52 motor-sensory (18.6%), 10 motor-sensory-interneuron (3.6%) 19 motor-interneuron (6.8%) and 53 motor (19%). They are connected by 3504 chemical synapses and 2086 electrical synapses. 26 neurons have been reported as having GABA as principal neurotransmitter, so their outward connections are considered inhibitory (Fig. 14b).

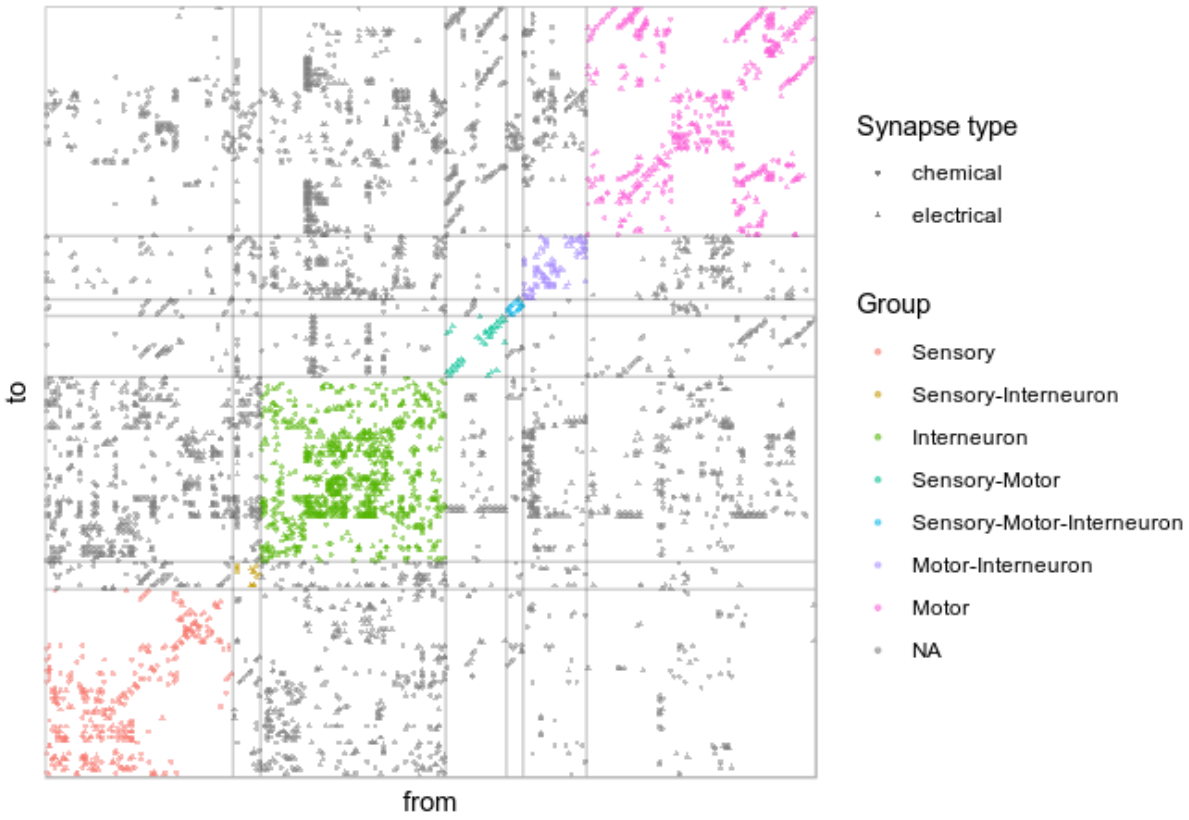

Figure 14a. Structural connectivity matrix for Somatic system. Colour coded for cell types' connections.

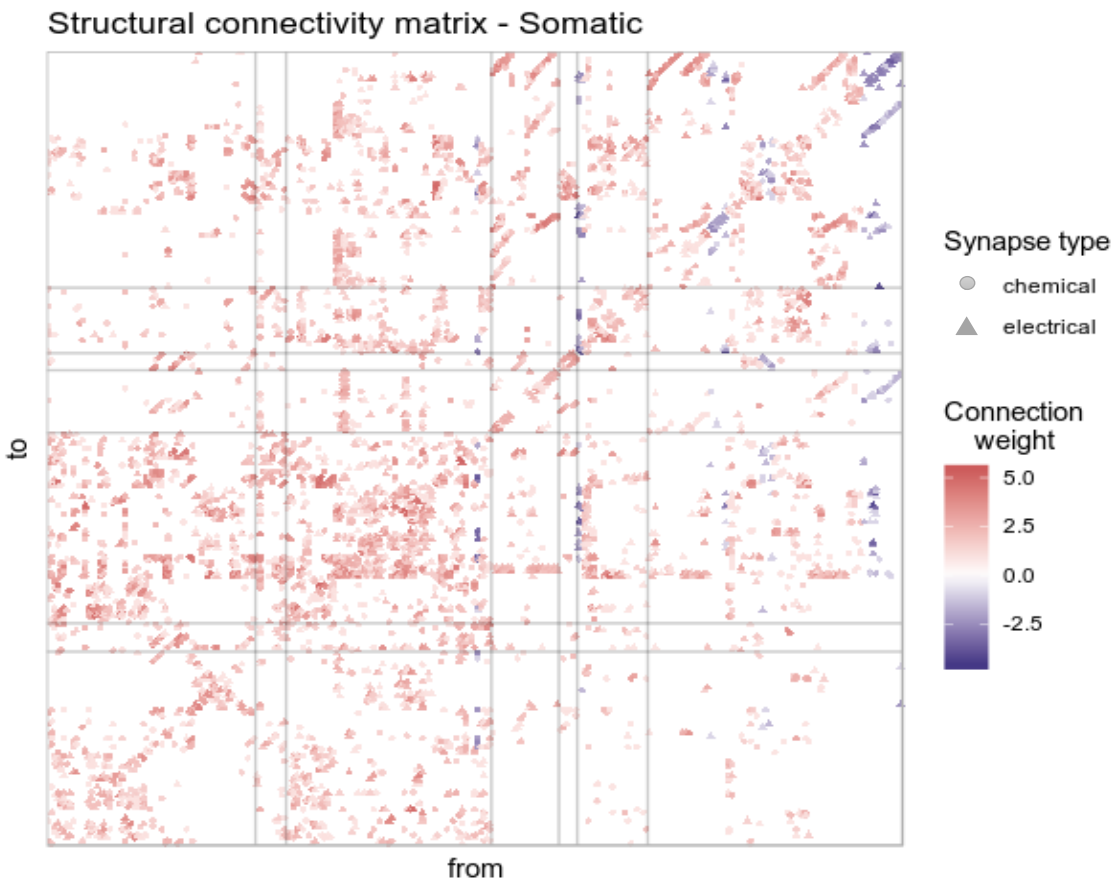

Figure 14b. Structural connectivity matrix for Somatic system. Colour coded for structural weight.

After more than two weeks of parallelized computing and after removing self-connections I obtained a functional network for somatic system (Fig. 15). In this case, because of the number of neurons it becomes difficult to get information directly from the plot.

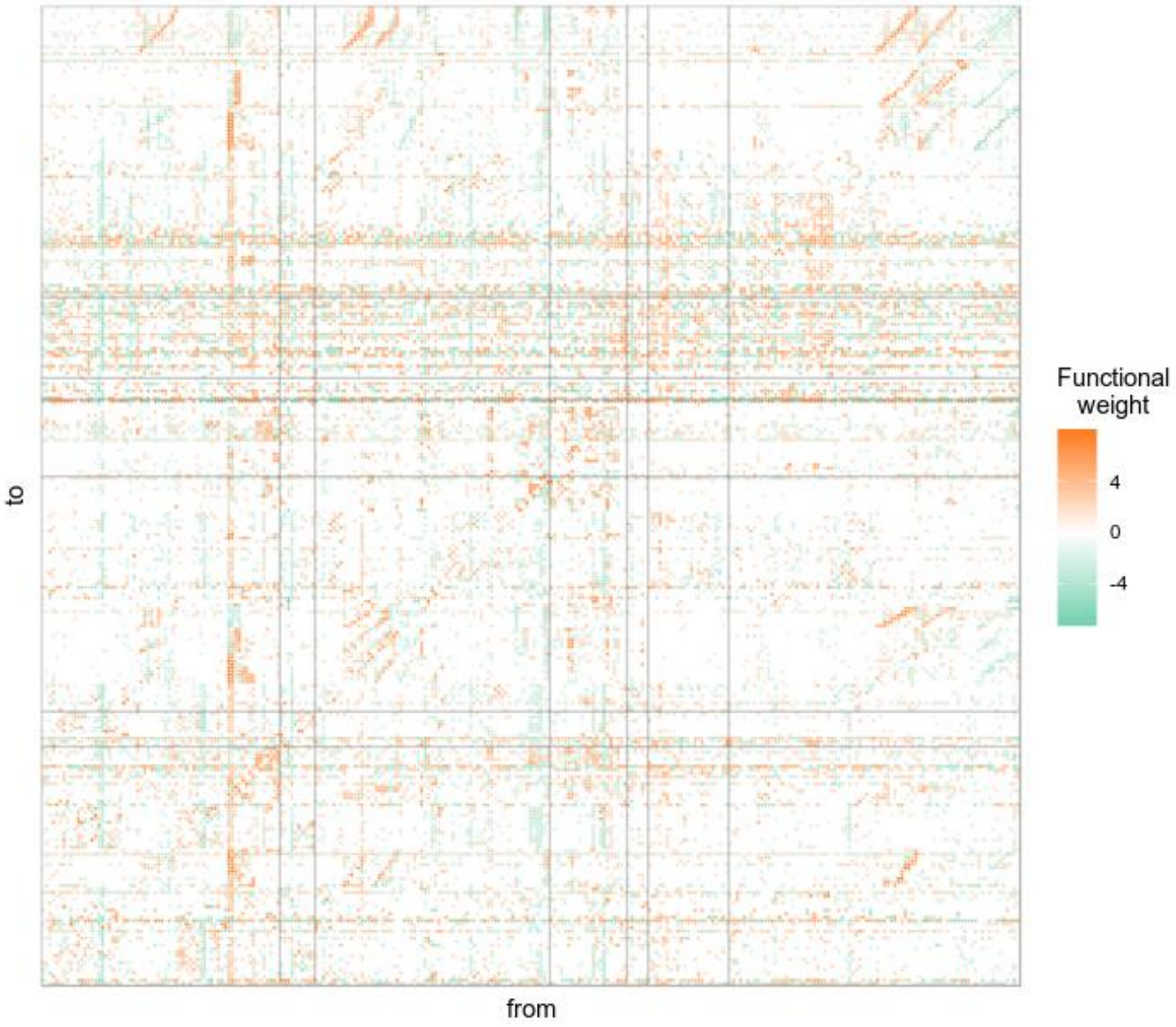

Figure 15. Somatic functional network. Colour coding weights in a logarithmic scale.

In terms of the categorical analysis of connections' existence (Table 3), I explored Granger Causality analysis predictions: excitatory structural connections showed sensitivity = 0.611 and specificity = 0.881; Inhibitory structural connections showed sensitivity = 0.781 and specificity = 0.855; and absence of structural connection showed sensitivity = 0.74 and specificity = 0.782. The categorical correlation with this variables structure was statistically significant with Chi-squared = 9578.2, df = 4, $p < 2.2 \times 10^{-16}$. This supports again our **second hypothesis** for somatic system about the categorical correlation between the existence of connections in the structural and functional networks.

Table 3. Adjacency matrix for structural – functional connections in somatic system.

		Structural connections			
		Excitatory	*Non-Existent*	*Inhibitory*	*Total*
Functional connections	*Positive r*	2812	8633	16	11393
	Null	1019	53646	40	54705
	Negative r	771	10422	200	11461
	Total	4602	72701	256	77559

Second, I calculated linear regressions for the relationships between structural and functional weights for the inhibitory and excitatory well predicted connections. Inhibitory connections showed a positive, moderate and statistically significant correlation (Fig. 16A): r= 0.34, 95% CI = [0.21, 0.45], t = 5.083, df = 198, p = 8.577×10^{-7}. Excitatory connections showed a slightly lower and statistically significant correlation (Fig. 16B): r = 0.314, 95% CI = [0.28, 0.35], t = 17.541, df = 2810, p < 2.2×10^{-16}. In this case, we can support our **third hypothesis** for somatic system about the correlation between structural and functional weights for both inhibitory and excitatory connections.

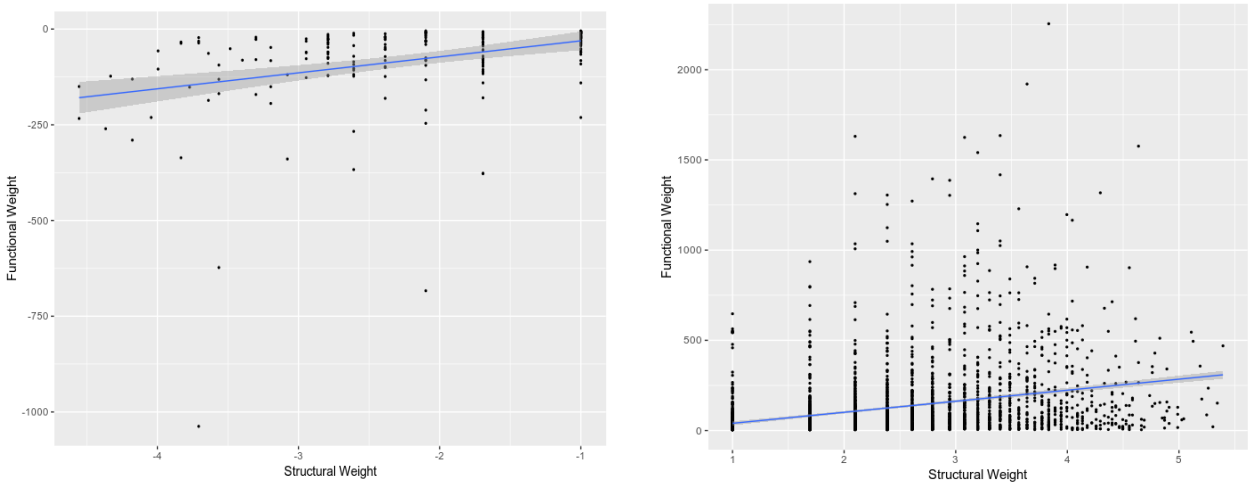

Figure 16. Weight correlations in somatic system for inhibitory synapses (left) and excitatory synapses (right). Points as connections and a linear regression curve fitted to them.

As with pharyngeal system, I differentiated here for electrical and chemical synapses. I found that taken independently both correlations were lower (Table 4), and that as in pharyngeal analysis, electrical weights were better predicted than chemical ones. The correlation for electrical and excitatory synapses was r = 0.21, 95% CI = [0.169, 0.27], t = 8.49, df = 1426, $p < 2.2x10^{-16}$. For chemical and excitatory: r = 0.079, 95% CI = [0.034, 0.123], t = 3.468, df = 1918, p = 0.0005. For electrical and inhibitory synapses: r = 0.30, 95% CI = [0.15, 0.449], t = 3.822, df = 140, p = 0.000199. For chemical and inhibitory: r = 0.172, 95% CI = [-0.0269, 0.3585], t = 1.715, df = 96, p = 0.09.

Table 4. Correlations table by connections type and network. Just showing statistically significant correlations. N.S. as not significant.

		Correlation	
		Excitatory	Inhibitory
Somatic	Whole	0.314	0.34
	Electrical	0.21	0.30
	Chemical	0.079	N.S.

Finally, I differentiated electrical and chemical categorical analysis (Table 5). For electrical network, excitatory connections had sensitivity = 0.752 and specificity = 0.881, inhibitory connections had sensitivity = 0.781 and specificity = 0.858, non-existent connections had sensitivity = 0.738 and specificity = 0.858. Categorical correlation was significant with Chi-squared = 7289.4, df = 4, $p < 2.2x10^{-16}$.

For chemical network, excitatory connections had sensitivity = 0.574 and specificity = 0.881, inhibitory connections had sensitivity = 0.781 and specificity = 0.854, non-existent connections had sensitivity = 0.738 and specificity = 0.767. Categorical correlation was also significant with Chi-squared = 6767.2, df = 4, $p < 2.2x10^{-16}$.

Table 5. Sensitivity and specificity in somatic system by network.

	Sensitivity			**Specificity**		
	Excitatory	*Null*	*Inhibitory*	*Excitatory*	*Null*	*Inhibitory*
Whole	0.611	0.738	0.781	0.881	0.782	0.855
Electrical	0.752	0.738	0.781	0.881	0.858	0.858
Chemical	0.574	0.738	0.781	0.881	0.767	0.855

Discussion

Structural and functional networks were not identical in our explorations; indeed, they were quite different albeit correlated in different ways. On one hand, where there was an excitatory connection in structural network, between 60-70% of the times there were also a functional connection. On the other hand, within that 60-70% of connections, weights were moderately correlated (when statistically significant): r = 0.31 and r = 0.34 in somatic system excitatory and inhibitory connections respectively.

I could also appreciate that the more connections in the analysis the closer both networks became. Correlations and categorical measures were higher in somatic system than in pharynx. This contradicts our fourth hypothesis that the more complexity in the network the lower the correlation. But I think this was a consequence of an interaction between Granger analysis and simulated activity, and not because of a reduction in complexity and indirect activity pathways. Few nodes in the network might have determine a poor activity dynamic simulation and thus, introduce error in Granger calculations. Having more nodes to compare with, Granger analysis algorithm becomes more sensible to connectivity. Further research should explore how number of nodes in the network is related to the correlations between structural and functional networks. How many nodes are needed to obtain significant correlations? Is there any number of nodes that maximize them?

Also, the differences between electrical and chemical networks were remarkable. I think it is related to the differences I implemented in our simulation models for both connection types. I wonder what specific parts of those models could be generating this phenomenon and how. Is that phenomenon related to the analysis of real neural activity recordings?

The main message of the study is that structural and functional networks are different although correlated. Why does this happen? As argued in the introduction, activity flowing over a structural neural network can take several pathways (some of them indirect), such that eventually two neurons that are not structurally connected tend to fire in sequence. This means that functional patterns can differ from underpinning structural ones. Does that mean that a single structure can give rise to different functional activity dynamics? I think so, I think that some structures might be able to support a greater number of functional dynamics. To what extent do structures differ in their capacity to accommodate different functional patterns? How can we measure the level of “flexibility” a structure could have to do it?

These might be future research questions to explore. First, using simple structures – with less than ten nodes- to observe and describe theoretical indirect pathways that could be found in a network. How those

simple indirect pathways would shape a functional network? Second, finding ways to measure them systematically. And third, once we can do it, explore how information processing, cognition and behaviour could be affected by different degrees of structural "flexibility".

With respect to our methodologies, I used a logarithmic **transformation of weights** to correct positive kurtosis in weight distribution (Fig. 1). This decision was made after the exploration of first network simulations with original weights. What I obtained were activity dynamics in which few nodes - targets of the highest weighted connections - were activated with much more frequency than the rest. Manipulating the synaptic efficacy coefficient, we could make every node to participate in the network dynamics but with an obvious overactivation in the network. On the other hand, I could make the network show moderate levels of activity but with scarce participation of most nodes (low-weighted connections). Validation proofs for this decision were the subsequent representations of activity I obtained with a strong similarity to electrophysiological recordings.

Regarding these **representations** (Fig. 3) in which simulated cycles (of 4 timesteps) seem to be similar to biological cycles (166 ms), it raises the question whether there could be a temporal match between them. This would mean in our model, that chemical synapses are effective (reaching postsynaptic neuron's body) approximately 166 ms after activation in presynaptic neuron's body (following our estimations from Nguyen et al. (2016) recordings). In addition, each timestep would represent 41.5 ms, the time that an electrical connection would last to be effective.

As noted in the introduction, *C. elegans* neurons' do not fire action potentials, but they have graded potentials (Goodman et al., 1998). Electrophysiological studies with current clamp recordings (Shindou et al., 2019) show that depolarization and recovery processes can take around 200 ms to be completed. In addition, C. elegans neurons' axons are not myelinated (Oikonomou & Shaham, 2011) what could delay information transmission. Considering the abstraction needed to build these models, these evidence could partially support our timeframes.

Network characterization was a description of our simulators' parameters behaviour over relevant activity dynamics variables. This helped us choosing sets of optimal parameters to generate coherent

activity for the following Granger Causality analysis. Synaptic efficacy that mediates the transformation of structural weights to cell depolarization was overall the most important parameter for the different variables measured. In addition, attenuation coefficient that mediates synaptic inputs from neighbour neurons had an expected influence over attenuated potentials. Less expected was its influence over minimum node activity, proposing that over a threshold where every neuron can be activated (that depends on synaptic efficacy), attenuation coefficient modulate the amount of minimum node activity.

I could observe a differential relevance of *Psens* parameter in pharyngeal (less influence) and somatic systems (more influence). I think it is due to a differential probability of *one* neuron to be stimulated in those systems, as that probability is linked to the number of sensors (the more sensors the more chances to obtaining one sensor activated). Thus, somatic system has higher probability of *one* sensor to be activated. The same happens with sensor-type groups and location subgroups. This difference is a caveat of our model that should be corrected in further developments of the simulator. It could be done by implementing as a factor of a static activation probability, the number of groups, subgroups and sensors in each stage of algorithm decision.

Additionally, I claimed above that our compartmentalization of sensory stimulation makes sensory input more coherent. Although, it is a better approach than complete randomized stimulation, it is not a final solution and I should find a better way of introducing environmental inputs in our simulator.

In general terms, I am aware that the abstraction in **our simulator** (avoiding the modelling of intracellular and molecular dynamics) could be generating a biased network activity that may be interacting *a posteriori* with Granger Causality analysis and, therefore, biasing results.

Our model doesn't implement the possibility of neuron hyperpolarization. Integrals of neighbours' activity inputs are used just to check threshold exceeding. This integral can be either positive or negative but just reaching threshold it has an effect over neurons activity. Thus, inhibitory process could be specially biased within our simulator and analysis.

To implement inhibitory processes and maintain point process modelling analysis, we could include another discrete state of activity under resting potential at -70mV. We should research what would be the most convenient voltage under -70mV to abstract a hyperpolarization state.

As commented earlier, *C. elegans* neurons have graded potentials but our model implements an integrate and fire model similar to spiking. Depolarization in a network with graded potentials is led by the amount of depolarization of sensory neurons and the strength of connections. Less connected neurons can depolarize although with less intensity, as they don't need to exceed a threshold.

Besides the questions stated above, **further research** should be done with the whole neural network (302 neurons) to analyse what difference introduce splitting of both systems and analysing them separately. Do the two neurons that link both systems have an impact on activity dynamics and subsequently on functional network?

Also, the questions developed here should be tackled from a biological approach. Using as activity measures accurate cellular recordings from *C. elegans* neurons, in which we could identify each C. elegans neurons.

This work emerged from questioning a possible near future when research in connectomics will have concrete claims about how specific neural structures are correlated with cognitive processes, personalities and disorders, and functional researchers will also have posed their own ideas about how activity dynamics are correlated with them. At that point, I would have some questions. First, the one I tried to answer here. How are structural and functional networks related? From our results, I could say that they are similar but not identical.

I would also wonder how "flexible" a structural connectivity pattern can be to give rise to different functional activity dynamics, and how "flexible" are different structural connectivity patterns to give rise to the same specific functional activity dynamic. Could it be that for some cognitive processes, network structures are not flexible enough so structure alone can determine processing throughputs? Could it be that for other cognitive processes structure is not determinant because it is so flexible that it can give rise to different functional patterns? Might that flexibility tell us something about adaptative neural processing? Might that flexibility be related to schizophrenia, creativity or dementia somehow?

References

Altun, Z. F., & Hall, D. H. (2011). Nervous system, general description. In *WormAtlas*. https://doi.org/10.3908/wormatlas.1.18

Atwood, H. L., & Karunanithi, S. (2002). Diversification of synaptic strength: Presynaptic elements. *Nature Reviews Neuroscience*, *3*(7), 497–516. https://doi.org/10.1038/nrn876

Azulay, A., Itskovits, E., & Zaslaver, A. (2016). The C. elegans Connectome Consists of Homogenous Circuits with Defined Functional Roles. *PLoS Computational Biology*, *12*(9), 1–16. https://doi.org/10.1371/journal.pcbi.1005021

Bargmann, C. I., & Marder, E. (2013). From the connectome to brain function. *Nature Methods*, *10*(6), 483–490. https://doi.org/10.1038/nmeth.2451

Bassett, D. S., & Sporns, O. (2017). Network neuroscience. *Nature Neuroscience*, *20*(3), 353–364. https://doi.org/10.1038/nn.4502

Branco, T., Marra, V., & Staras, K. (2010). Examining size-strength relationships at hippocampal synapses using an ultrastructural measurement of synaptic release probability. *Journal of Structural Biology*, *172*(2), 203–210. https://doi.org/10.1016/j.jsb.2009.10.014

Bullmore, E., & Sporns, O. (2009). Complex brain networks: graph theoretical analysis of structural and functional systems. *Nature Reviews. Neuroscience*, *10*(3), 186–198. https://doi.org/10.1038/nrn2575

Cao, Z. (2017). *Information flow in the neuronal network of C . elegans and analysis of its dynamic oscillatory activity with transfer entropy*. University of Edinburgh. Retrieved from github.com/zaleCao/elegansNet

Catani, M., & Ffytche, D. H. (2005). The rises and falls of disconnection syndromes. *Brain*, *128*(10), 2224–2239. https://doi.org/10.1093/brain/awh622

Delbeuck, X., Van der Linden, M., & Collete, F. (2003). Alzheimer's Disease as a Disconnection Syndrome? *Neuropsychology Review*, *13*(2), 79–92.

Ford, J. H., & Kensinger, E. A. (2014). The relation between structural and functional connectivity

depends on age and on task goals. *Frontiers in Human Neuroscience*, *8*(May), 1–12. https://doi.org/10.3389/fnhum.2014.00307

Friston, K., Brown, H. R., Siemerkus, J., & Stephan, K. E. (2016). The dysconnection hypothesis (2016). *Schizophrenia Research*, *176*(2–3), 83–94. https://doi.org/10.1016/j.schres.2016.07.014

Galán, R. F. (2008). On How Network Architecture Determines the Dominant Patterns of Spontaneous Neural Activity. *PLoS ONE*, *3*(5), e2148. https://doi.org/10.1371/journal.pone.0002148

Gleeson, P., Lung, D., Grosu, R., Hasani, R., & Larson, S. D. (2018). c302: a multiscale framework for modelling the nervous system of Caenorhabditis elegans. *Philosophical Transactions of the Royal Society B: Biological Sciences*, *373*(1758), 20170379. https://doi.org/10.1098/rstb.2017.0379

Goodman, M. B., Hall, D. H., Avery, L., & Lockery, S. (1998). Active currents regulate sensitivity and dynamic range in C. elegans neurons. *Neuron*, *20*, 763–772. Retrieved from http://www.wormbase.org/db/misc/paper?name=WBPaper00003059

Greicius, M. D., Supekar, K., Menon, V., & Dougherty, R. F. (2009). Resting-state functional connectivity reflects structural connectivity in the default mode network. *Cerebral Cortex*, *19*(1), 72–78. https://doi.org/10.1093/cercor/bhn059

Honey, C. J., Sporns, O., Cammoun, L., Gigandet, X., Thiran, J. P., Meuli, R., & Hagmann, P. (2009). Predicting human resting-state functional connectivity from structural connectivity. *Proceedings of the National Academy of Sciences*, *106*(6), 2035–2040. https://doi.org/10.1073/pnas.0811168106

Jarrell, T. A., Wang, Y., Bloniarz, A. E., Brittin, C. A., Xu, M., Thomson, J. N., … Emmons, S. W. (2012). The Connectome of a Decision-Making Neural Network. *Science*, *337*(6093), 437–444. https://doi.org/10.1126/science.1221762

Johansen-Berg, H. (2013). Human connectomics - What will the future demand? *NeuroImage*, *80*, 541–544. https://doi.org/10.1016/j.neuroimage.2013.05.082

Kim, S., Putrino, D., Ghosh, S., & Brown, E. N. (2011). A Granger Causality Measure for Point Process Models of Ensemble Neural Spiking Activity. *PLoS Computational Biology*, *7*(3), e1001110. https://doi.org/10.1371/journal.pcbi.1001110

Loer, C., & Rand, J. (2016). The Evidence for Classical Neurotransmitters in Caenorhabditis elegans. In *WormAtlas*. https://doi.org/10.3908/wormatlas.5.200

Mellem, J. E., Brockie, P. J., Madsen, D. M., & Maricq, A. V. (2009). Reply to “First report of action potentials in a C. elegans neuron is premature.” *Nature Neuroscience*, *12*(4), 366–366. https://doi.org/10.1038/nn0409-366

Nguyen, J. P., Shipley, F. B., Linder, A. N., Plummer, G. S., Liu, M., Setru, S. U., … Leifer, A. M. (2016). Whole-brain calcium imaging with cellular resolution in freely behaving Caenorhabditis elegans. *Proceedings of the National Academy of Sciences*, *113*(8), E1074–E1081. https://doi.org/10.1073/pnas.1507110112

Oikonomou, G., & Shaham, S. (2011). The Glia of Caenorhabditis elegans. *Glia*, *59*(9), 1253–1263. https://doi.org/10.1002/glia.21084

Park, H. J., & Friston, K. (2013). Structural and functional brain networks: From connections to cognition. *Science*, *342*(6158). https://doi.org/10.1126/science.1238411

Pereira, L., Kratsios, P., Serrano-saiz, E., Sheftel, H., Mayo, A. E., Hall, D. H., … Hobert, O. (2015). A cellular and regulatory map of the cholinergic nervous system of C . elegans. *ELIFE*, 1–46. https://doi.org/10.7554/eLife.12432.001

Perrone, D., Sullivan, C. J., Pratt, T. C., & Margaryan, S. (2004). Parental Efficacy, Self-Control, and Delinquency: A Test of a General Theory of Crime on a Nationally Representative Sample of Youth. *International Journal of Offender Therapy and Comparative Criminology*, *48*(3), 298–312. https://doi.org/http://dx.doi.org/10.1177/0306624X03262513

Pozo, K., & Goda, Y. (2010). Unraveling Mechanisms of Homeostatic Synaptic Plasticity. *Neuron*, *66*(3), 337–351. https://doi.org/10.1016/j.neuron.2010.04.028

Sanz-Arigita, E. J., Schoonheim, M. M., Damoiseaux, J. S., Rombouts, S. A. R. B., Maris, E., Barkhof, F., … Stam, C. J. (2010). Loss of “Small-World” Networks in Alzheimer’s Disease: Graph Analysis of fMRI Resting-State Functional Connectivity. *PLoS ONE*, *5*(11). https://doi.org/10.1371/journal.pone.0013788

Schafer, W. (2006). Neurophysiological methods in C. elegans: an introduction. *WormBook*. https://doi.org/10.1895/wormbook.1.111.1

Seung, H. S. (2011). Towards functional connectomics. *Nature*, *471*(7337), 171–172. https://doi.org/10.1038/471170a

Shindou, T., Ochi-Shindou, M., Murayama, T., Saita, E., Momohara, Y., Wickens, J. R., & Maruyama, I. N. (2019). Active propagation of dendritic electrical signals in C. elegans. *Scientific Reports*, *9*(1), 3430. https://doi.org/10.1038/s41598-019-40158-9

Siegelbaum, S. A., & Kandel, E. R. (2013). Overview of synaptic transmission. In *Principles of Neural Science* (Fifth, pp. 177–188). New York: McGraw-Hill.

Sporns, O. (2011a). *Networks of the brain*. Cambridge: MIT Press.

Sporns, O. (2011b). The human connectome: A complex network. *Annals of the New York Academy of Sciences*, *1224*(1), 109–125. https://doi.org/10.1111/j.1749-6632.2010.05888.x

Sporns, O. (2013). The human connectome: Origins and challenges. *NeuroImage*, *80*, 53–61. https://doi.org/10.1016/j.neuroimage.2013.03.023

Uddin, L. Q. (2013). Complex relationships between structural and functional brain connectivity. *Trends in Cognitive Sciences*, *17*(12), 600–602. https://doi.org/10.1016/j.tics.2013.09.011

Van Essen, D. C., & Ugurbil, K. (2012). The future of the human connectome. *NeuroImage*, *62*(2), 1299–1310. https://doi.org/10.1016/j.neuroimage.2012.01.032

Varshney, L. R., Chen, B. L., Paniagua, E., Hall, D. H., & Chklovskii, D. B. (2011). Structural properties of the Caenorhabditis elegans neuronal network. *PLoS Computational Biology*, *7*(2). https://doi.org/10.1371/journal.pcbi.1001066

Watts, D. J., & Strogatz, S. H. (1998). Collective dynamics of “small-world” networks. *Nature*, *393*(6684), 440–442.

White, J. G., Southgate, E., Thomson, J. N., & Brenner, S. (1986). The Structure of the Nervous System of the Nematode Caenorhabditis elegans. *Philosophical Transactions of the Royal Society B: Biological Sciences*, *314*(1165), 1–340. https://doi.org/10.1098/rstb.1986.0056

Yuste, R. (2015). From the neuron doctrine to neural networks. *Nature Reviews Neuroscience*. Nature Publishing Group. https://doi.org/10.1038/nrn3962

Atwood, H. L., & Karunanithi, S. (2002). Diversification of synaptic strength: Presynaptic elements. *Nature Reviews Neuroscience*, *3*(7), 497–516. https://doi.org/10.1038/nrn876

Azulay, A., Itskovits, E., & Zaslaver, A. (2016). The C. elegans Connectome Consists of Homogenous Circuits with Defined Functional Roles. *PLoS Computational Biology*, *12*(9), 1–16. https://doi.org/10.1371/journal.pcbi.1005021

Bargmann, C. I., & Marder, E. (2013). From the connectome to brain function. *Nature Methods*, *10*(6), 483–490. https://doi.org/10.1038/nmeth.2451

Bassett, D. S., & Sporns, O. (2017). Network neuroscience. *Nature Neuroscience*, *20*(3), 353–364. https://doi.org/10.1038/nn.4502

Branco, T., Marra, V., & Staras, K. (2010). Examining size-strength relationships at hippocampal synapses using an ultrastructural measurement of synaptic release probability. *Journal of Structural Biology*, *172*(2), 203–210. https://doi.org/10.1016/j.jsb.2009.10.014

Bullmore, E., & Sporns, O. (2009). Complex brain networks: graph theoretical analysis of structural and functional systems. *Nature Reviews. Neuroscience*, *10*(3), 186–198. https://doi.org/10.1038/nrn2575

Cao, Z. (2017). *Information flow in the neuronal network of C . elegans and analysis of its dynamic oscillatory activity with transfer entropy*. University of Edinburgh.

Catani, M., & Ffytche, D. H. (2005). The rises and falls of disconnection syndromes. *Brain*, *128*(10), 2224–2239. https://doi.org/10.1093/brain/awh622

Delbeuck, X., Van der Linden, M., & Collete, F. (2003). Alzheimer's Disease as a Disconnection Syndrome? *Neuropsychology Review*, *13*(2), 79–92.

Ford, J. H., & Kensinger, E. A. (2014). The relation between structural and functional connectivity depends on age and on task goals. *Frontiers in Human Neuroscience*, *8*(May), 1–12. https://doi.org/10.3389/fnhum.2014.00307

Friston, K., Brown, H. R., Siemerkus, J., & Stephan, K. E. (2016). The dysconnection hypothesis (2016). *Schizophrenia Research*, *176*(2–3), 83–94. https://doi.org/10.1016/j.schres.2016.07.014

Galán, R. F. (2008). On How Network Architecture Determines the Dominant Patterns of Spontaneous Neural Activity. *PLoS ONE*, *3*(5), e2148. https://doi.org/10.1371/journal.pone.0002148

Goodman, M. B., Hall, D. H., Avery, L., & Lockery, S. (1998). Active currents regulate sensitivity and dynamic range in C. elegans neurons. *Neuron*, *20*, 763–772. Retrieved from

http://www.wormbase.org/db/misc/paper?name=WBPaper00003059

Greicius, M. D., Supekar, K., Menon, V., & Dougherty, R. F. (2009). Resting-state functional connectivity reflects structural connectivity in the default mode network. *Cerebral Cortex*, *19*(1), 72–78. https://doi.org/10.1093/cercor/bhn059

Honey, C. J., Sporns, O., Cammoun, L., Gigandet, X., Thiran, J. P., Meuli, R., & Hagmann, P. (2009). Predicting human resting-state functional connectivity from structural connectivity. *Proceedings of the National Academy of Sciences*, *106*(6), 2035–2040. https://doi.org/10.1073/pnas.0811168106

Jarrell, T. A., Wang, Y., Bloniarz, A. E., Brittin, C. A., Xu, M., Thomson, J. N., … Emmons, S. W. (2012). The Connectome of a Decision-Making Neural Network. *Science*, *337*(6093), 437–444. https://doi.org/10.1126/science.1221762

Johansen-Berg, H. (2013). Human connectomics - What will the future demand? *NeuroImage*, *80*, 541–544. https://doi.org/10.1016/j.neuroimage.2013.05.082

Kim, S., Putrino, D., Ghosh, S., & Brown, E. N. (2011). A Granger Causality Measure for Point Process Models of Ensemble Neural Spiking Activity. *PLoS Computational Biology*, *7*(3), e1001110. https://doi.org/10.1371/journal.pcbi.1001110

Loer, C., & Rand, J. (2016). The Evidence for Classical Neurotransmitters in Caenorhabditis elegans. In *WormAtlas*. https://doi.org/10.3908/wormatlas.5.200

Mellem, J. E., Brockie, P. J., Madsen, D. M., & Maricq, A. V. (2009). Reply to "First report of action potentials in a C. elegans neuron is premature." *Nature Neuroscience*, *12*(4), 366–366. https://doi.org/10.1038/nn0409-366

Nguyen, J. P., Shipley, F. B., Linder, A. N., Plummer, G. S., Liu, M., Setru, S. U., … Leifer, A. M. (2016). Whole-brain calcium imaging with cellular resolution in freely behaving Caenorhabditis elegans. *Proceedings of the National Academy of Sciences*, *113*(8), E1074–E1081. https://doi.org/10.1073/pnas.1507110112

Park, H. J., & Friston, K. (2013). Structural and functional brain networks: From connections to cognition. *Science*, *342*(6158). https://doi.org/10.1126/science.1238411

Pereira, L., Kratsios, P., Serrano-saiz, E., Sheftel, H., Mayo, A. E., Hall, D. H., … Hobert, O. (2015). A cellular and regulatory map of the cholinergic nervous system of C . elegans. *ELIFE*, 1–46.

https://doi.org/10.7554/eLife.12432.001

Perrone, D., Sullivan, C. J., Pratt, T. C., & Margaryan, S. (2004). Parental Efficacy, Self-Control, and Delinquency: A Test of a General Theory of Crime on a Nationally Representative Sample of Youth. *International Journal of Offender Therapy and Comparative Criminology*, *48*(3), 298–312. https://doi.org/http://dx.doi.org/10.1177/0306624X03262513

Sanz-Arigita, E. J., Schoonheim, M. M., Damoiseaux, J. S., Rombouts, S. A. R. B., Maris, E., Barkhof, F., … Stam, C. J. (2010). Loss of "Small-World" Networks in Alzheimer's Disease: Graph Analysis of fMRI Resting-State Functional Connectivity. *PLoS ONE*, *5*(11). https://doi.org/10.1371/journal.pone.0013788

Schafer, W. (2006). Neurophysiological methods in C. elegans: an introduction. *WormBook*. https://doi.org/10.1895/wormbook.1.111.1

Seung, H. S. (2011). Towards functional connectomics. *Nature*, *471*(7337), 171–172. https://doi.org/10.1038/471170a

Shindou, T., Ochi-Shindou, M., Murayama, T., Saita, E., Momohara, Y., Wickens, J. R., & Maruyama, I. N. (2019). Active propagation of dendritic electrical signals in C. elegans. *Scientific Reports*, *9*(1), 3430. https://doi.org/10.1038/s41598-019-40158-9

Siegelbaum, S. A., & Kandel, E. R. (2013). Overview of synaptic transmission. In *Principles of Neural Science* (Fifth, pp. 177–188). New York: McGraw-Hill.

Sporns, O. (2011a). *Networks of the brain*. Cambridge: MIT Press.

Sporns, O. (2011b). The human connectome: A complex network. *Annals of the New York Academy of Sciences*, *1224*(1), 109–125. https://doi.org/10.1111/j.1749-6632.2010.05888.x

Sporns, O. (2013). The human connectome: Origins and challenges. *NeuroImage*, *80*, 53–61. https://doi.org/10.1016/j.neuroimage.2013.03.023

Uddin, L. Q. (2013). Complex relationships between structural and functional brain connectivity. *Trends in Cognitive Sciences*, *17*(12), 600–602. https://doi.org/10.1016/j.tics.2013.09.011

Van Essen, D. C., & Ugurbil, K. (2012). The future of the human connectome. *NeuroImage*, *62*(2), 1299–1310. https://doi.org/10.1016/j.neuroimage.2012.01.032

Varshney, L. R., Chen, B. L., Paniagua, E., Hall, D. H., & Chklovskii, D. B. (2011). Structural properties of the Caenorhabditis elegans neuronal network. *PLoS Computational Biology*, *7*(2). https://doi.org/10.1371/journal.pcbi.1001066

Watts, D. J., & Strogatz, S. H. (1998). Collective dynamics of "small-world" networks. *Nature*, *393*(6684), 440–442.

White, J. G., Southgate, E., Thomson, J. N., & Brenner, S. (1986). The Structure of the Nervous System of the Nematode Caenorhabditis elegans. *Philosophical Transactions of the Royal Society B: Biological Sciences*, *314*(1165), 1–340. https://doi.org/10.1098/rstb.1986.0056

Yuste, R. (2015). From the neuron doctrine to neural networks. *Nature Reviews Neuroscience*. Nature Publishing Group. https://doi.org/10.1038/nrn3962